

# Inhomogeneous excitonic superfluid in balanced and imbalanced bilayer quantum Hall systems: Mutual Composite Fermion and composite Boson approaches

Jinwu Ye

Department of Physics, The Pennsylvania State University, University Park, PA, 16802  
(February 24, 2019)

We develop both Mutual Composite Fermion (MCF) and Composite Boson (CB) approach to study balanced and imbalanced Bilayer Quantum Hall systems (BLQH) and make critical comparisons between the two approaches. We find the CB approach is superior to the MCF approach in the BLQH with broken symmetry. By using this CB theory, we are able to put spin and charge degrees of freedom in the same footing, explicitly bring out the spin-charge connection and classify all the possible excitations in a systematic way. We first study the balanced BLQH and re-derive many previous results in a simple and transparent way. Then we push the CB theory further to study the instability driven by magneto-roton minimum collapsing at a finite wavevector in the pseudo-spin channel which leads to the formation of inhomogeneous exciton pairing. We propose there are two critical distances  $d_{c1} < d_{c2}$  and three phases as the distance increases. When  $0 < d < d_{c1}$ , the system is in the well known exciton superfluid (ESF) state, when  $d_{c1} < d < d_{c2}$ , the system is in the inhomogeneous Exciton superfluid (I-ESF) state, there is a first order transition at  $d_{c1}$  driven by the collapsing of magneto-roton minimum in the pseudo-spin channel. The charge sector remains gapped in the I-ESF phase, so is still a QH state. When  $d_{c2} < d < 1$ , the system becomes two weakly coupled  $\nu = 1/2$  Composite Fermion Fermi Liquid (FL) state. There is also a first order transition at  $d = d_{c2}$ . However, disorders could smear the two first order transitions into two second order transitions. Due to the pairing modulation in the I-ESF, its superfluid density is very small compared to the ESF, its corresponding KT transition temperature is also small, this state is more vulnerable to disorders. This ground state may be true ground state and is the origin of excess dissipations observed in both interlayer tunneling and counterflow experiments. While the ESF state only happens at experimentally inaccessible small distance. This I-ESF may resolve many discrepancies between experimental observations and the previous theories. Then we study the effects of imbalance on both ESF, I-ESF and FL states. Finally, we compare our results with the previous results achieved from the LLL+HF approach, the other proposals on the possible intermediate phases and available experimental data.

## I. INTRODUCTION

Extensive attention has been lavished on Fractional Quantum Hall Effects (FQHE) in multicomponent systems since the pioneering work by Halperin [1]. These components could be the spins of electrons when the Zeeman coupling is very small or layer indices in multilayered system. In particular, spin-polarized Bilayer Quantum Hall systems at total filling factor  $\nu_T = 1$  have been under enormous experimental and theoretical investigations over the last decade [2]. When the interlayer separation  $d$  is sufficiently large, the bilayer system decouples into two separate compressible  $\nu = 1/2$  layers. Earlier experiments exhibited a strong suppression of the tunneling current at low biases [3]. However, when  $d$  is smaller than a critical distance  $d_c$ , even in the absence of interlayer tunneling, the system undergoes a quantum phase transition into a novel spontaneous interlayer coherent incompressible phase [2]. At low temperature, with extremely small interlayer tunneling amplitude, Spielman et al discovered a very pronounced narrow zero bias peak in this interlayer coherent incompressible state [4]. M. Kellbgg et al also observed quantized Hall drag resistance at  $h = e^2$  [5]. In recent counterflow experiments, it was found that both linear longitudinal and

Hall resistances take activated forms and vanish only in the low temperature limit [6].

Starting from Halperin's 111 wavefunction which describes a bi-layer system with  $N_1$  ( $N_2$ ) electrons in the top (bottom) layer (the total number of electrons is  $N = N_1 + N_2$ ), using various methods, several authors discovered a Neutral Gapless Mode (NGM) with linear dispersion relation  $\epsilon = \hbar v k$  and that there is a finite temperature Kosterlitz-Thouless (KT) phase transition associated with this NGM [7-9]. By treating the two layer indices as two pseudo-spin indices, Girvin, MacDonald and collaborators mapped the bilayer system into a Easy Plane Quantum Ferromagnet (EPQFM) [10,11,2]. They established the mapping by projecting the Hamiltonian of the BLQH onto the Lowest Landau Level (LLL) and then using subsequent Hartree-Fock (HF) approximation and gradient expansion (called LLL+HF in the following). In the picture of EPQFM [2], the canonical ensemble with definite  $S^z = N_1 - N_2 = 0$  is replaced by Grand canonical ensemble with fluctuating  $S^z$ . The relative fluctuation of  $S^z$  is at the order of  $1/\sqrt{N} \rightarrow 0$  as  $N \rightarrow \infty$ . By drawing the analogy with superconductivity where canonical ensemble with definite number of Cooper pairs is shown to be equivalent to BCS wavefunction which is a grand canonical ensemble with in-

definite number of Cooper pairs, the authors in [10,11,2] argued this trial wavefunction is a good approximation to the exact ground state. The low energy excitations above the ground state is given by an effective 2 + 1 dimensional XY model. There are 4 flavors of topological defects called "merons" which carry fractional charges  $\pm 1/2$  and also have vorticities. They have logarithmic divergent self energies and are bound into pairs at low temperature. The lowest energy excitations carry charge  $\pm e$  which are a meron pair with opposite vorticity and the same charge. There is a finite temperature phase transition at  $T_{KT}$  where bound states of the 4 flavors of merons are broken into free merons. The large longitudinal resistivity ( $\sim 1k\Omega$ ) observed in [4] at very low temperature indicated that these meron pairs are highly mobile. In the presence of small tunneling, they [10,2] found that when the applied in-plane magnetic field is larger than a critical field  $B_{jj}$ , there is a phase transition from a commensurate state to an incommensurate state (C-IC) with broken translational symmetry. When  $B > B_{jj}$ , there is a finite temperature KT transition which restores the translation symmetry by means of dislocations in the domain wall structure in the incommensurate phase. Starting from the EPQFM approach, several groups investigated I-V curves in the presence of small tunneling [12]. In addition to the work mentioned above, there are also many other works done on BLQH. For example, several authors applied different versions of composite fermion Chern-Simons theory to study BLQH systems in [14,15,17].

Despite the intensive theoretical research in [7,11,2], there are many open problems. According to the present theories, in the ESF, there should be the interlayer tunneling Josephson effect, finite temperature KT transition and vanishing linear longitudinal and Hall resistances in the counterflow channel below the KT transition temperature. Unfortunately, all these characteristics have never been observed in the experiments. For example, although it appears certain that the dramatic conductance peak observed at  $d < d_c$  is due to the collective NGM in the ESF state, no theory can explain the magnitude of zero bias peak conductance which, though enormously enhanced, does not exceed  $10^{-2} \frac{e^2}{h}$ , its width and its dependence on proximity to the ESF state boundary (see, however, the most recent work [13]). All the previous calculations predicted that the in-plane field will split the zero bias peak into two side peaks, but the experiments showed that although there are two tiny shoulders appearing, the central peak stays. The excess dissipation observed in the counterflow experiments [6] appears to vanish only as  $\ln T \rightarrow 0$  limit. The origin of the excess dissipation remains an important unresolved question. In short, what is the real ground state at  $d < d_c$  remains mysterious.

In this paper, we use both Mutual Composite Fermion

(MCF) [28-30] and Composite Boson (CB) approaches [33,34] to study balanced and imbalanced BLQH systems. We identify many problems with MCF approach. Then we develop a simple and effective CB theory which naturally avoids all the problems suffered in the MCF approach. The CB theory may also be applied to study the possible novel intermediate phases between the exciton superfluid (ESF) at very small distance and the Fermi Liquid (FL) state at very large distance and the quantum phase transitions between these different ground states. Therefore the CB approach is superior to the MCF approach in the BLQH with broken symmetry. By using this CB theory, we are able to put spin and charge degree freedoms in the same footing, explicitly bring out the spin-charge connection and classify all the possible excitations in a systematic way. We first study the balanced BLQH and re-derive many previous results in a simple and transparent way. We also make detailed comparisons with the EPQFM calculations and point out the limitations of the CB approach. Then we push the CB theory further to study the density wave instability at a finite wavevector in the pseudo-spin channel which leads to the formation of inhomogeneous exciton pairing. For balanced BLQH, there are two critical distances  $d_{c1} < d_{c2}$ . When  $0 < d < d_{c1}$ , the system is in the ESF state, when  $d_{c1} < d < d_{c2}$ , the system is in the inhomogeneous Exciton superfluid (IESF) state, there is a first order transition at  $d_{c1}$  driven by the collapsing of magnetoroton minimum in the pseudo-spin channel. The charge sector remains gapped in both ESF and the IESF phases, so the system shows QHE effects in both phases. When  $d_{c2} < d < 1$ , the system becomes two weakly coupled  $\nu = 1/2$  Composite Fermion Fermi Liquid (CFFL) state. There is a also first order transition at  $d = d_{c2}$ . However, disorders could smear the two first order transitions into two second order transitions. Then we study the effects of imbalance on both the ESF and the IESF. We find that as we increase the imbalance, the system supports continuously changing fractional charges, the spin-wave velocity decreases quadratically, the meron pair separation stays the same, while the critical in-plane magnetic field for the Commensurate-Incommensurate transition increases, the critical distance  $d_{c1}$  between the ESF and the IESF decreases. On the disordered FL side, the imbalance could drive a quantum phase transition from the FL to the IESF. We also discuss briefly the effects of disorders and compare our results with the previous results achieved from the LLL+HF approach, the other proposals on the possible intermediate phases and available experimental data.

The EPQFM approach is a microscopic one which takes care of LLL projection from the very beginning. However, the charge sector was explicitly projected out, the connection and coupling between the charge sector which displays Fractional Quantum Hall effect and the spin sector which displays interlayer phase coherence was

not obvious in this approach. While in the CB theory, it is hard to incorporate the LLL projection (see however [31]), some parameters can only be taken as phenomenological parameters to be fitted into the microscopic LLL+HF calculations or experimental data as discussed in section III A-2. It is an effective low energy theory, special care is needed to capture some physics at microscopic length scales. The two approaches are complementary to each other.

The analogy of homogeneous pairing between the electron-electron Cooper pairing in superconductor and the electron-hole exciton pairing in the BLQH was first realized by Fertig in [7] and pushed further by Girvin, MacDonald and collaborators in [10,11,2]. As shown in this paper, the homogeneous pairing leading to the ESF phase is stable only at very small distance  $d < d_{c1}$ . At intermediate distance  $d_{c1} < d < d_{c2}$ , an inhomogeneous pairing state becomes possible. Before getting into details of BLQH, it is insightful to draw some analogy on inhomogeneous pairing between the two systems. In conventional BCS superconductors, an electron with spin up is paired with its partner with spin down across the Fermi surface to form a Cooper pair with total momentum zero. Now one applies a magnetic field to split the spin up and spin down electron Fermi surfaces by the Zeeman effect. For s-wave superconductor, if the Zeeman splitting is very small compared to the gap, then the superconducting state is stable, if it is much larger than the gap, then it will break the Cooper pairs and turn the superconducting state into a normal state. When it is comparable to the gap  $\phi_0$  at zero magnetic field, it may become non-trivial, a new state may intervene. About 40 years ago, Fulde and Ferrell [19], Larkin and Ovchinnikov [20], pointed out that an inhomogeneous superconductor with pairing order parameter oscillating in space may be the ground state at a narrow window of Zeeman splitting  $\mu_B = \frac{\phi_0}{2} < \mu_B < \frac{\phi_0}{2} \cdot 0.754$  [21,19,20] (Fig. 4). This inhomogeneous state is called LOFF state where the Cooper pairs carry finite momentum. It breaks both the U(1) gauge symmetry and the translational order. Unfortunately, the LOFF state has never been observed in conventional superconductors, because in these systems, the Zeeman effect is too small and is overwhelmed by orbital effects. There are at least three crucial differences between the superconductor and the BLQH (1) The former is a P-P pairing leading to a Cooper pair, while the latter is a P-H pairing leading to an exciton. (2) The former breaks a gauge U(1) symmetry, resulting no Goldstone modes at  $k = 0$  due to the Higgs Mechanism, while the latter breaks a global U(1) symmetry in the pseudo-spin sector resulting a Goldstone mode at  $k = 0$ . So the exciton pairing contains both  $k = 0$  pairing and finite momentum pairing, while the LOFF pairing only contains the finite momentum pairing. (3) The Zeeman field splits the spin up and spin down Fermi spheres, therefore affects the pairing in P-P channel di-

rectly. However, the imbalance in BLQH will not affect the pairing in P-H channel directly, because the number of electrons in the top layer are always equal to that of holes in the bottom layer independent of the imbalance. So the Zeeman field in SC and the imbalance in BLQH play completely different role. The evolution sequence of ESF-IESF-FL as distance increases in BLQH resembles the sequence of SC-LOFF-FL in superconductors as the Zeeman field increases with the distance playing the role of the Zeeman field. Although the LOFF pairing in the P-P channel has not been firmly established in any superconductors yet, as shown in this paper, the inhomogeneous pairing in the P-H channel could be firmly established in electron-hole systems like BLQH, because there is no such analog of the annoying orbital effects in the BLQH. Due to the DW formation in the IESF, its superfluid density is very small compared to the ESF, its corresponding KT transition temperature is also small, this new ground state is more vulnerable to disorders. This ground state may be the origin of excess dissipations observed in both interlayer tunneling and counterflow experiments. While the ESF state only happens at experimentally inaccessible small distance.

Consider a bi-layer system with  $N_1$  ( $N_2$ ) electrons in top (bottom) layer and with interlayer distance  $d$  in the presence of magnetic field  $B = r \cdot A$ :

$$\begin{aligned} H &= H_0 + H_{int} \\ H_0 &= \sum_{\alpha} \int d^2x c_{\alpha}^{\dagger}(\mathbf{x}) \left( \frac{i\hbar \nabla + \frac{e}{c} A(\mathbf{x})}{2m} \right)^2 c_{\alpha}(\mathbf{x}) \\ H_{int} &= \frac{1}{2} \sum_{\alpha} \int d^2x d^2x^0 c_{\alpha}^{\dagger}(\mathbf{x}) V(\mathbf{x} - \mathbf{x}^0) c_{\alpha}(\mathbf{x}^0) \end{aligned} \quad (1)$$

where electrons have bare mass  $m$  and carry charge  $e$ ,  $c_{\alpha}; = 1, 2$  are electron operators in top and bottom layers,  $c_{\alpha}^{\dagger}(\mathbf{x}) = c_{\alpha}^{\dagger}(\mathbf{x}) c_{\alpha}(\mathbf{x})$ ;  $n_{\alpha}; = 1, 2$  are normal ordered electron densities on each layer. The intralayer interactions are  $V_{11} = V_{22} = \frac{e^2}{r}$ , while interlayer interaction is  $V_{12} = V_{21} = \frac{e^2}{r^2 + d^2}$  where  $\epsilon$  is the dielectric constant. For imbalanced bi-layers,  $n_1 \neq n_2$ , but the background positive charges are still the same in the two layers, the chemical potential term is already included in  $H_{int}$  in Eqn.1.

The rest of the paper is organized as follows. In section II, we use a MCF theory to study the BLQH. We achieve some success, but also run into many troublesome problems. In section III, we use a CB theory which puts spin and charge sector on the same footing to study the BLQH. We demonstrate why this CB theory naturally avoid all the problems suffered in the MCF approach. We also compare the CB approach with the EPQFM approach and point out advantages and limitations of both approaches. Most importantly, we push the CB theory further to analyze carefully the instability in the pseudo-spin channel which lead to the IESF state and study its properties at both zero and finite temperatures. Then

we study the effects of imbalance on ESF, IESF and FL states. In the final section, we summarized the main results of the paper and concluded that CB theory is superior to MCF approach in BLQH system with broken symmetry.

## II. MUTUAL COMPOSITE FERMION APPROACH: SUCCESS AND FAILURE

In parallel to advances in bi-layer QH systems, much progress has been made on novel physics involving quasi-particles and vortices in high temperature superconductors. Anderson employed a single-valued singular gauge transformation to study the quasi-particle energy spectrum in the vortex lattice state [23]. By employing the Anderson transformation, the author studied the quasi-particle transport in random vortex array in the mixed state [24]. Balents et al, investigated the zero temperature quantum phase transition from d-wave superconductor to underdoped side by assuming the transition is driven by the condensations of quantum fluctuation generated vortices [25,26]. The author extended the Anderson singular gauge transformation for static vortices to a mutual singular gauge transformation for quantum fluctuation generated dynamic vortices to study the novel interactions between quasi-particles and vortices near this quantum phase transition [26].

In this section, by employing essentially the same singular gauge transformation used to study the interactions between quasi-particles and vortices in high temperature superconductors, we revisit the bi-layer QH systems.

### (1) Singular Gauge Transformation:

Performing a single-valued singular gauge transformation (SGT) [26,27]:

$$U = e^{i\tilde{\alpha} \int d^2x \int d^2x^0 \tilde{\alpha}(\mathbf{x}) \arg(\mathbf{x} - \mathbf{x}^0) \tilde{\alpha}(\mathbf{x}^0)}; \quad \tilde{\alpha} = 1 \quad (2)$$

we can transform the above Hamiltonian into:

$$H_0 = \int d^2x \tilde{\psi}(\mathbf{x}) \frac{(-i\hbar \nabla + \frac{e}{c} \tilde{\mathbf{A}}(\mathbf{x}) - \hbar \mathbf{a}(\mathbf{x}))^2}{2m} \tilde{\psi}(\mathbf{x}) \quad (3)$$

where the transformed fermion is given by:

$$\begin{aligned} \tilde{\psi}_1(\mathbf{x}) &= U \psi_1(\mathbf{x}) U^{-1} = \psi_1(\mathbf{x}) e^{i \int d^2x^0 \arg(\mathbf{x} - \mathbf{x}^0) \tilde{\alpha}(\mathbf{x}^0)} \\ \tilde{\psi}_2(\mathbf{x}) &= U \psi_2(\mathbf{x}) U^{-1} = \psi_2(\mathbf{x}) e^{i \int d^2x^0 \arg(\mathbf{x}^0 - \mathbf{x}) \tilde{\alpha}(\mathbf{x}^0)} \end{aligned} \quad (4)$$

and the two mutual Chern-Simons (CS) gauge fields satisfy:  $\nabla \cdot \mathbf{a} = 0$ ;  $\nabla \cdot \mathbf{a} = 2 \tilde{\alpha}(\mathbf{x})$  (See Fig.1a). Obviously, the interaction term is unaffected by the singular-gauge transformation. Note that it is  $\arg(\mathbf{x} - \mathbf{x}^0)$  appearing in  $\tilde{\psi}_1(\mathbf{x})$ , while  $\arg(\mathbf{x}^0 - \mathbf{x})$  appearing in  $\tilde{\psi}_2(\mathbf{x})$  in Eqn.4. This subtle difference is crucial to prove all the commutation relations are kept intact by the single-valued singular gauge transformation Eqn.2. Note also that  $\arg(\mathbf{x}^0 - \mathbf{x})$  works equally well in Eqn.2.

It is easy to check that in single layer system where  $\tilde{\alpha}_1 = \tilde{\alpha}_2 = \tilde{\alpha}$ , Eqn.2 reduces to the conventional singular gauge transformation employed in [30]:

$$\tilde{\psi}_a(\mathbf{x}) = e^{i \int d^2x^0 \arg(\mathbf{x} - \mathbf{x}^0) \tilde{\alpha}(\mathbf{x}^0)} \psi_a(\mathbf{x}) \quad (5)$$

where  $\tilde{\psi}_a(\mathbf{x}) = \tilde{\psi}_a^\dagger(\mathbf{x}) \psi_a(\mathbf{x})$  is the electron density in layer  $a = 1, 2$ . It puts two flux quanta in the opposite direction to the external magnetic field at the position of each electron (Fig. 1b). On the average, a CF feels a reduced effective field which is the external magnetic field minus the attached flux quanta.

For  $\tilde{\alpha} = 1$  bi-layer system, Eqn.4 puts one flux quantum in one layer in the opposite direction to the external magnetic field at the position directly above or below each electron in the other layer (Fig.1a).

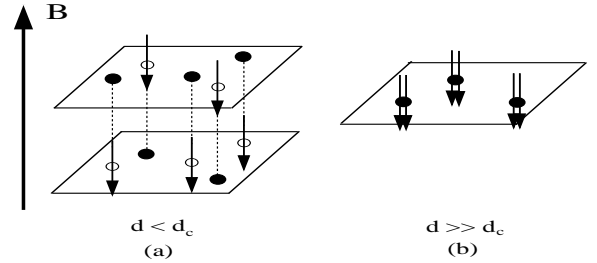


Fig 1: Contrast the flux attachment in Eqn.2 (a) with that in Eqn.5 (b). In (a), there is one flux quantum in layer 1 when there is an electron directly downstairs in layer 2 and there is one flux quantum in layer 2 when there is an electron directly upstairs in layer 1. One can compare Fig. 1a with Fig. 2. For simplicity, we only show three electrons in the top layer and two electrons in the bottom layer.

On the average, a Mutual Composite Fermion (MCF) in each layer feels a reduced effective field which is the external magnetic field minus the inserted flux quanta in this layer. In single layer system, it is essential to attach even number of flux quanta to keep Fermi statistics intact. The two attached flux quanta are moving together with the associated electron. However, in bi-layer system, inserting one flux quantum does keep Fermi statistics intact. The inserted one flux quantum in one layer is moving together with its associated electron in the other layer. If choosing  $\tilde{\alpha} = 1/2$ , the transformation is not single-valued, the statistics is changed from fermion to boson, this choice will be pursued in the next section on Composite boson approach.

### (2) Mean field theory:

In the following, we put  $\hbar = c = e = 1$ . At total filling factor  $\nu = 1$ ,  $\tilde{\alpha} = 2n$  where  $n = n_1 + n_2$  is the total average electron density. By absorbing the average values of C-S gauge fields  $\nabla \cdot \mathbf{a} = 2n$  into the external gauge potential  $\tilde{\mathbf{A}} = \mathbf{A} - \mathbf{a}$ , we have:

$$H_0 = \int d^2x \sum_{\mathbf{y}} \frac{(\mathbf{r} + \mathbf{A}(\mathbf{x}) - \mathbf{a}(\mathbf{x}))^2}{2m} \quad (\mathbf{x}) \quad (6)$$

where  $\mathbf{r} + \mathbf{A} = 2\pi\mathbf{n}$  and  $\mathbf{r} - \mathbf{a} = 2\pi\mathbf{m}$  ( $\mathbf{x}$ ) are the deviations from the corresponding average density. In the following, we will simply use  $\mathbf{a}$  to stand for these deviations).

When  $d < d_c$ , the strong inter-layer interactions renormalize the bare mass into two effective masses  $m$  [31]. MCF in each layer feel effective magnetic field  $B = r + A = 2\pi n$ , therefore fill exactly one MCF Landau level. The energy gaps are simply the cyclotron gaps of the MCF Landau levels  $\epsilon_c = \frac{B}{m}$ .

### (3) Fractional charges:

Let's look at the charge of quasi-particles created by MCF field operators  $\psi(\mathbf{x})$ . Intuitively, inserting  $\psi_1(\mathbf{x})$  on layer 1 not only inserts an electron in layer 1 at position  $\mathbf{x}$ , but also pushes  $n_2 = \frac{N_2}{N}$  electrons in layer 2 into its boundary, therefore induces a local charge deficit at  $\mathbf{x}$  in layer 2 which carries charge  $-n_2$ , the total charge at  $\mathbf{x}$  is  $e_1 = 1 + n_2 = -n_1$ . If  $\mathbf{x}$  and  $\mathbf{y}$  are two points far apart, then the product of operators  $\psi_1(\mathbf{x})\psi_1(\mathbf{y})$  in layer 1 will create a pair of fractional charges  $q_1$  at positions  $\mathbf{x}$  and  $\mathbf{y}$  with the charge gap  $h_{c1}$ . Similarly, inserting  $\psi_2(\mathbf{x})$  in layer 2 will create a charge  $e_2 = 1 + n_1 = -n_2$  at  $\mathbf{x}$  (note that  $e_1 + e_2 = 1$ ). The product of operators  $\psi_2(\mathbf{x})\psi_2(\mathbf{y})$  in layer 2 will create a pair of fractional charges  $q_2$  at  $\mathbf{x}$  and  $\mathbf{y}$  with the charge gap  $h_{c2}$ . Only when the two layers are identical  $N_1 = N_2$ ,  $e_1 = e_2 = 1/2$  which carries fractional charge of even denominators. In general, the imbalanced bilayer system supports continuously changing total fractional charges in the thermodynamic limit.

The above arguments give the correct total fractional charges  $q_1; q_2$ . However, it can not determine the relative charge distributions between the two layers. At mean field level, the energies of all the possible relative charge differences are degenerate. The lowest energy configuration can only be determined by fluctuations. The above arguments are at most intuitive. The much more rigorous and elegant topological arguments can only be given in the composite boson theory of the next section.

### (4) Fluctuations:

When considering fluctuations around the MCF mean field theory, it is convenient to go to Lagrangian [31]:

$$L = \sum_{\mathbf{y}} (\partial_{\mathbf{y}} \mathbf{a}_0)^2 + \sum_{\mathbf{y}} \frac{(\mathbf{r} + \mathbf{A} - \mathbf{a})^2}{2m} + i\mathbf{a}_0 \cdot \mathbf{n} + \frac{i\mathbf{q}}{2} (\mathbf{a}_0 - \mathbf{a}_t) + \frac{q}{4} (\mathbf{a}_t^1 \mathbf{a}_t^1 + \mathbf{a}_t^2 \mathbf{a}_t^2 + 2e^{-iqd} \mathbf{a}_t^1 \mathbf{a}_t^2) \quad (7)$$

where the constraints have been used to rewrite the Coulomb interactions and  $\mathbf{a}_t$  is the transverse spatial component of gauge field in Coulomb gauge  $\mathbf{r} \cdot \mathbf{a} = 0$  [30,32].

In Lorenz invariant gauge the second to the last term becomes the mutual C-S term  $\frac{1}{4} (\mathbf{a}_0 - \mathbf{a}_t)^2$  where  $\mathbf{a}_0, \mathbf{a}_t$  refer to layer indices, while  $\mathbf{r}, \mathbf{A}$  refer to space-time indices. The Hamiltonian has local  $U(1)_1 \times U(1)_2$  gauge symmetry which corresponds to the invariance under  $\psi(\mathbf{x}) \rightarrow e^{i\theta(\mathbf{x})} \psi(\mathbf{x}); \mathbf{a} \rightarrow \mathbf{a} + \partial \theta$ .

Integrating out MCF  $\psi_1; \psi_2$  to one-loop and carefully expanding the interlayer Coulomb interaction to the necessary order in the long-wavelength limit leads to:

$$L = \frac{i\mathbf{q}}{2} \mathbf{a}_0^+ \mathbf{a}_t^+ + \frac{q}{4} (\mathbf{a}_t^+)^2 + \frac{+}{4} \mathbf{q}^2 (\mathbf{a}_0^+)^2 + \frac{1}{4} (\mathbf{a}_0^+)^2 + (\mathbf{a}_0^+ + \frac{d}{2} \mathbf{q}^2) (\mathbf{a}_t^+)^2 + \frac{+}{4} \mathbf{q}^2 (\mathbf{a}_0^-)^2 + \frac{1}{4} (\mathbf{a}_0^-)^2 + (\mathbf{a}_0^- + \frac{d}{2} \mathbf{q}^2) (\mathbf{a}_t^-)^2 + \frac{1}{2} \mathbf{q}^2 \mathbf{a}_0^+ \mathbf{a}_0^- + \frac{1}{2} (\mathbf{a}_0^+)^2 + \mathbf{q}^2 \mathbf{a}_t^+ \mathbf{a}_t^- + \quad (8)$$

where  $\mathbf{a}_0^{\pm}$  are higher gradient terms and the transverse component of gauge field in Coulomb gauge  $\mathbf{r} \cdot \mathbf{a} = 0$  [30,32],  $\mathbf{a} = \mathbf{a}^1 + \mathbf{a}^2$  and  $\mathbf{a} = \frac{1}{2} (\mathbf{a}_1 - \mathbf{a}_2)$ ;  $\mathbf{a}^{\pm} = \frac{1}{2} (\mathbf{a}_1 \pm \mathbf{a}_2)$ .  $\mathbf{a}^+$  ( $\mathbf{a}^-$ ) stands for the total (relative) density fluctuation.  $\mathbf{a}$  is the NGM identified previously [7(9)]. The dielectric constants  $\epsilon = \frac{m}{2B}$  and the susceptibilities  $\chi = \frac{1}{2m}$  were calculated in single layer system in [29].

The first two terms are C-S term and Coulomb interaction term for + gauge field which take exactly the same forms as in a single layer system [30,32]. The third and the fourth terms are non-relativistic Maxwell terms for + and - modes respectively. The last two terms couple + mode to - mode. Integrating out + modes leads to  $\frac{1}{2} \mathbf{q}^2 (\mathbf{a}_0^-)^2 + (\mathbf{a}_0^- + \frac{d}{2} \mathbf{q}^2) (i\mathbf{q}_0 \mathbf{a}_t^-)$  which are sub-leading to the Maxwell term of  $\mathbf{a}_0; \mathbf{a}_t$ . In fact, these terms break Time reversal and Parity, in principle, a C-S term  $i\mathbf{q}_0 \mathbf{a}_t$  will be generated under RG sense. However, the coefficient of this generated C-S term could be so small that it can be neglected except at experimentally unattainable low temperatures.

### (5) Neutral Gapless modes:

For simplicity, we only consider the balanced case and will comment on imbalanced case later. Note that  $\mathbf{r} \cdot \mathbf{a} = 2\pi\mathbf{n}$  where  $\mathbf{n} = \mathbf{n}_2(\mathbf{x}) - \mathbf{n}_1(\mathbf{x})$  is the relative density fluctuation of the two layers. Introducing a variable  $\theta$  which is conjugate to  $\mathbf{n}(\mathbf{x})$ , namely  $[\theta(\mathbf{x}); \mathbf{n}(\mathbf{x})] = i(\mathbf{x} \cdot \mathbf{x})$ , we can write a spin-wave Hamiltonian density:

$$H = \frac{1}{2} \sum_{\mathbf{s}} (\dot{\theta})^2 + \frac{1}{2} \sum_{\mathbf{s}} (\mathbf{r} \cdot \mathbf{a})^2 \quad (9)$$

If  $\theta$  is treated as a continuous variable, then  $\theta$  is a free field varying from  $-\infty$  to  $\infty$ . By integrating out  $\theta$ , we get the representation:

$$L = \frac{1}{2} \sum_{\mathbf{s}} (\partial_{\mathbf{y}} \mathbf{a})^2 + \frac{1}{2} \sum_{\mathbf{s}} (\mathbf{r} \cdot \mathbf{a})^2 \quad (10)$$

Integrating out  $\phi$ , we get an effective action density in the  $\phi$  representation which is dual to the above representation:

$$L = \frac{1}{2} \sum_s \phi^2 + \frac{1}{2} \sum_s \left( \frac{\phi}{q} \right)^2 \quad (11)$$

Plugging the constraint  $r = a = 2$  into Eqn.11, we get:

$$L_a = \frac{1}{2} \left( \sum_s \phi^2 + \sum_s \phi^2 \right) (a_t)^2 \quad (12)$$

This is consistent with the well-known fact that a pure  $2+1$  dimensional  $U(1)$  gauge field is dual to a  $2+1$  dimensional Gaussian model which does not have any topological excitations [56]. Comparing Eqn.12 with Eqn.8 (for simplicity, we take  $N_1 = N_2$ ), we get  $\phi_s = h_c^2$ ;  $\phi_s = [2^2 (\frac{d}{2})]^{-1}$ . So the spin stiffness scales as the cyclotron gap and the finite charge gap of MCF implies finite spin stiffness. In order to compare with experimental data in [4,5], we have to put back  $h_c$ ;  $e$ ; and find the spin-wave velocity:

$$v^2 = \frac{(\phi_c)^2}{n} + \left( \frac{c}{l} \right) \left( \frac{d}{1} \right) \frac{\phi_c}{2n} \quad (13)$$

where  $n$  is the total density,  $l$  is the magnetic length and  $1/l = 137$  is the fine structure constant. Note that the correct expansion of interlayer Coulomb interaction is crucial to get the second term.

By measuring the transport properties at finite temperature, the authors in [5] found the activation gap  $E_A = 0.4K$ . By setting  $E_A = h_c^2$  and plugging the experimental parameters  $n = 5.2 \times 10^{10} \text{ cm}^{-2}$ ;  $d = 1 = 1.61$ ;  $\phi_s = 12.6$  into Eqn.13, we find that the first term is  $1.65 \times 10^{10} (\text{cm}^{-2})^2$ , the second term is  $2.54 \times 10^{12} (\text{cm}^{-2})^2$  which is two orders of magnitude bigger than the first term. Finally, we find  $v = 1.59 \times 10^6 \text{ cm/s}$  which is dominated by the second term. This value is in good agreement with  $v = 1.4 \times 10^6 \text{ cm/s}$  found in [4].

#### (6) Topological excitations:

As discussed in the previous paragraph, at mean field theory, there are four kinds of gapped excitations with total fractional charges  $q_1 = \frac{1}{2}$  and  $q_2 = \frac{1}{2}$  which, for example, can be excited by finite temperature close to  $h_c^2$ . But their relative charge distributions between the two layers are undetermined. In fact, all the possible excitations can be characterized by their  $(a^+; a^-)$  charges  $(q_1; q_2)$ . For example, the four kinds of excitations are denoted by  $(\frac{1}{2}; \frac{1}{2})$ ;  $(\frac{1}{2}; -\frac{1}{2})$ ;  $(-\frac{1}{2}; \frac{1}{2})$ ;  $(-\frac{1}{2}; -\frac{1}{2})$ . For  $q_1 = q_2$ , they reduce to two sets:  $(\frac{1}{2}; \frac{1}{2})$ . If  $\phi$  in Eqn.9 is treated as a discrete variable, then  $0 < \phi < 2\pi$  is an angle variable.  $q$  must be integers  $0; \pm 1; \pm 2, \dots$ . Exchanging leads to  $1/r$  interaction between the four sets of beasts. While exchanging  $a$  leads to logarithmic interactions which lead to a bound state between two beasts with opposite  $q \neq 0$ . The energy of this bound state with length  $L$  is

$E_b = \frac{1}{2} \left( \frac{1}{L} + \frac{1}{L} \right) + q_1^2 \frac{e^2}{L} + q_2^2 \frac{e^2}{L} \ln L = 1$  where  $\frac{1}{2}$  and  $\frac{1}{L}$  are the core energies of QH and QP respectively.

An important question to ask is what is the gluing conditions (or selection rules) of  $(q_1; q_2)$  for the realizable excitations? Namely, what is spin  $(q_1)$  and charge  $(q_2)$  connection? Two specific questions are: (1) Is there a charge neutral vortex excitation with  $(0; \frac{1}{2})$ ? Being charge neutral, this kind of excitation is a bosonic excitation. (2) Is there a charge  $1=2$  and spin neutral excitation  $(\frac{1}{2}; 0)$ ? If they do exist, then the QP and QH pair with  $q = 0$  have the lowest energy  $h_c^2 = \frac{1}{2} + \frac{1}{2}$ . They decouple from a gauge field, therefore interact with each other only with  $1/r$  interaction and are asymptotically free even at  $T = 0$  just like those in single layer system. Their charges are evenly distributed in the two layers (namely carry fractional charges  $1=4$  in each separate layer). They are deconfined  $1=2$  excitations which are completely different excitations from merons which are confined logarithmically.

Unfortunately, the spin-charge connection is far from obvious in this MCF approach. So little can be said about these two possibilities. In the composite boson approach to be presented in the next section, both interesting possibilities are ruled out.

#### (7) Extension to other filling factors:

Let's briefly discuss  $\nu = 1=2$  bilayer system. It is well known that this state is described by Halperin's 331 state [4]. In this state, the singular gauge transformation  $U = e^{i \int d^2x \int d^2x^0 U(\mathbf{x}) \arg(\mathbf{x} - \mathbf{x}^0) (\mathbf{x}^0)}$  where the matrix  $U = \frac{1}{2} \begin{pmatrix} 2 & 1 \\ 1 & 2 \end{pmatrix}$  attached two intralayer flux quanta and one interlayer flux quantum to electrons to form Entangled Composite Fermions (ECF). At layer 1 (layer 2), the filling factor of ECF is  $\nu_1 = \frac{N_1}{N_2}$  ( $\nu_2 = \frac{N_2}{N_1}$ ). Only when the two layers are identical  $N_1 = N_2$ , we get  $\nu_1 = \nu_2 = 1$  QH states on both layers, therefore  $\nu = 1=2$  system lacks interlayer coherence.

#### (8) Comparison with another version of CF approach:

It is instructive to compare our MCF picture developed in this section with the earlier pictures proposed in [15]. When  $N_1 = N_2$ , the authors in [15] attached  $\sim 2$  flux quanta of layer 2 to electrons in layer 1 or vice versa to form interlayer composite fermions so that at mean field theory, CF in each layer form a compressible Fermi liquid. They conjectured that a gauge field fluctuation mediates an attractive interaction between CF in different layers which leads to a (likely p-wave) pairing instability. This pairing between CF in different layers opens an energy gap. But no systematic theory is developed along this picture. In the MCF picture studied in this section, there is a charge gap which is equal to the cyclotron gap even at mean field theory which is robust against any gauge field fluctuation. Due to using  $\sim 2$ , the authors in [16] concluded that the mutual Hall drag resistivity is  $2h/e^2$  which is inconsistent with the exper-

experimental result in [5].

(9) Interlayer tunneling:

The interlayer tunneling term is:

$$H_t = t c_1^y(\mathbf{x}) c_2(\mathbf{x}) + h.c. \quad (14)$$

Substituting Eqn.4 into above equation leads to:

$$H_t = t \frac{y}{1}(\mathbf{x}) e^{i \int d^2 x^0 [\arg(\mathbf{x}^0) - \arg(\mathbf{x}^0)]} c_2(\mathbf{x}) + h.c. \quad (15)$$

This is a very awkward equation to deal with.

The authors in [8] pointed out that the tunneling process of an electron from one layer to the other corresponds to an instanton in the  $2+1$  dimensional compact QED. They applied the results of Polyakov on instanton-anti-instanton plasma on  $2+1$  dimensional compact QED and found the effective action:

$$L = \frac{1}{g^2} (\partial_\mu \theta)^2 + \frac{t}{2\pi} \cos \theta \quad (16)$$

where  $g$  is the  $U(1)$  gauge coupling constant given in Eqn.10. In the original work of Polyakov,  $\theta$  is a non-compact field  $-\pi < \theta < \pi$ . The compactness of  $\theta$  was forced in an ad hoc way in [8]. Note that the compactness of QED has nothing to do with the compactness of  $\theta$ .

(10) Summary of limited success of MCF theory:

We use a Mutual Composite Fermion (MCF) picture to explain the interlayer coherent incompressible phase at  $d < d_c$ . This MCF is a generalization of Composite Fermion (CF) in single layer QH systems to bilayer QH systems [28,30,29,31]. In the mean field picture, MCF in each layer is exactly  $\nu = 1$  MCF Landau level. There are four kinds of gapped quasi-particles (QP) and quasi-holes (QH) with total fractional charges  $q_1 = \frac{1}{2}$ ;  $q_2 = \frac{1}{2}$  (For  $\nu_1 = \nu_2 = 1/2$ , they reduce to two sets). When considering the fluctuations above the  $\nu = 1$  MCF QH states, we identify the NGM with linear dispersion relation  $\omega = vk$  and determine  $v$  in terms of experimental measurable quantities. When interpreting the activation gap  $E_A$  found in [5] in terms of the cyclotron gap of the  $\nu = 1$  MCF Landau level, we calculate  $v$  and find its value is in good agreement with the value determined in [4]. Tentatively, we intend to classify all the possible excitations in terms of  $a^+$  and  $a^-$  charges ( $q_+; q_-$ ).

(11) Serious problems with MCF approach:

Despite the success of the MCF approach mentioned above, there are many serious drawbacks of this approach. We list some of them in the following.

(a) The determination of the fractional charges is at most intuitive. A convincing determination can only be firmly established from the CB approach to be discussed in the next section. Furthermore, the MCF still carries charge 1, while the QP or QH carry charge  $\nu = 2$ . An

extension of Murthy-Shankar formalism [31] in SLQH to BLQH may be needed to express physics in terms of these  $\nu = 2$  QP and QH.

(b) It is easy to see that the spin wave dispersion in Eqn.13 remains linear  $\omega = vk$  even in the  $d \rightarrow 0$  limit. This contradicts with the well established fact that in the  $d \rightarrow 0$  limit, the linear dispersion relation will be replaced by quadratic Ferromagnetic spin-wave dispersion relation  $\omega = k^2$  due to the enlarged  $SU(2)$  symmetry at  $d \rightarrow 0$ . This is because the flux attachment singular gauge transformation Eqn.2 breaks  $SU(2)$  symmetry at very beginning even in the  $d \rightarrow 0$  limit.

(c) The broken symmetry in the ground state is not obvious without resorting to the (111) wavefunction. The physics of exciton pairing can not be captured. The origin of the gapless mode is not clear.

(d) The compactness of the angle  $\theta$  in Eqn.10 was put in by hand in an ad hoc way.

(e) The spin-charge connection in  $(q_+; q_-)$  can not be determined.

(f) The interlayer tunneling term can not be derived in a straight-forward way. See section III-E.

(g) In the imbalanced case, there are two MCF cyclotron gaps  $\hbar\omega_c$  at mean field theory. However, there is only one charge gap in the system. It is not known how to reconcile this discrepancy within MCF approach.

(h) It is not known how to push the MCF theory further to study the very interesting and novel inhomogeneous exciton superfluid state to be discussed in III-B.

In the following, we will show that the alternative CB approach not only can achieve all the results in this section, but also can get rid of all these drawbacks naturally. Most importantly, it can be used to address the novel state: inhomogeneous exciton superfluid state in intermediate distances.

### III. COMPOSITE BOSON APPROACH

Composite boson approach originated from Girvin and MacDonald's off-diagonal long range order [33], formulated in terms of Chern-Simons Ginsburg-Landau theory [34]. It has been successfully applied to Laughlin's series  $\nu = \frac{1}{2s+1}$  [34] and  $\nu = 1$  spin unpolarized QH system [35]. It has also been applied to BLQH [9,11]. Unfortunately, it may not be applied to study Jain's series at  $\nu = \frac{p}{2sp+1}$  with  $p \neq 1$  and  $\nu = 1/2$  Fermi liquid system. In this section, we applied CSG L theory to study imbalanced bi-layer QH system. Instead of integrating out the charge degree of freedom which was done in all the previous CB approach [9,10], we keep charge and spin degree of freedom on the same footing and explicitly stress the spin and charge connection. We study how the imbalance affects various physical quantities such as spin wave velocity, the meron pair distance and energy, the critical





Note that in Eqn 24 both  $\psi_+$  and  $\psi_-$  couple to terms with two spatial gradients, therefore can be dropped relative to the terms in Eqn 23 which contains just one temporal gradient.

In the following, we will discuss balanced and imbalanced cases separately:

A . Balanced case  $\mu_1 = \mu_2 = 1/2$ : excitonic superfluid state

Putting  $\mu_1 = \mu_2 = 1/2$  and  $h_z = 0$  into Eqn 23, we get the Lagrangian in the balanced case:

$$\begin{aligned} L = & i \psi_+^\dagger \left( \frac{1}{2} \partial_t^2 + a_0 \right) \psi_+ + \frac{1}{2m} \left( \frac{1}{2} r^2 + a^2 \right) \psi_+^\dagger \psi_+ \\ & + \frac{1}{2} \psi_+^\dagger V_+ (\mathbf{q}) \psi_+ + \frac{i}{2} a_0 (r^2 + a^2) \psi_+^\dagger \psi_+ \\ & + \frac{i}{2} \psi_-^\dagger \partial_t^2 \psi_- + \frac{1}{2m} \left( \frac{1}{2} r^2 \right) \psi_-^\dagger \psi_- + \frac{1}{2} V_- (\mathbf{q}) \psi_-^\dagger \psi_- \end{aligned} \quad (25)$$

In the balanced case, the symmetry is enlarged to  $U(1)_L \times U(1)_R \times Z_2$  where the global  $Z_2$  symmetry is the exchange symmetry between layer 1 and layer 2. At temperatures much lower than the vortex excitation energy, we can neglect vortex configurations in Eqn 25 and only consider the low energy spin-wave excitation. The charge sector ( $\psi_+$  mode) and spin sector ( $\psi_-$  mode) are essentially decoupled.

(1)  $O(3)$ -diagonal algebraic order in the charge sector:

The charge sector is essentially the same as the CSGL action in BLQH. Using the constraint  $a_t = \frac{2}{q} \psi_+^\dagger \psi_+$ , neglecting vortex excitations in the ground state and integrating out  $\psi_+$  leads to the effective action of  $\psi_-$ :

$$L_c = \frac{1}{8} + (\mathbf{q}; !)_- \left[ \frac{!^2 + \frac{1}{q^2}}{V_+ (\mathbf{q}) + \frac{4}{m} \frac{1}{q^2}} \right] + (\mathbf{q}; !)_- \quad (26)$$

where  $!^2 = !_c^2 + \frac{1}{m} q^2 V_+ (\mathbf{q})$  and  $!_c = \frac{2}{m}$  is the cyclotron frequency.

From Eqn 26, we can find the equal time correlator of  $\psi_-$ :

$$\begin{aligned} \langle \psi_-^\dagger (\mathbf{q}) \psi_- (\mathbf{q}) \rangle &= \sum_{\mathbf{l}} \frac{d!}{2} \langle \psi_-^\dagger (\mathbf{q}; !)_- (\mathbf{q}; !)_- \rangle \\ &= 2 \frac{2}{q^2} + O\left(\frac{1}{q}\right) \end{aligned} \quad (27)$$

which leads to the algebraic order:

$$\langle e^{i(\psi_+^\dagger(\mathbf{x}) - \psi_+^\dagger(\mathbf{y}))} \rangle = \frac{1}{\mathcal{K} \frac{1}{y^2}} \quad (28)$$

Note that if we define  $\tilde{\psi}_+ = \frac{1}{\sqrt{2}} \psi_+ = \psi_+ / \sqrt{2}$ , then  $\langle e^{i(\tilde{\psi}_+^\dagger(\mathbf{x}) - \tilde{\psi}_+^\dagger(\mathbf{y}))} \rangle = \frac{1}{\mathcal{K} \frac{1}{y^{3/2-2}}} \frac{1}{y^{3/2-2}}$  which takes exactly the same form as that in  $\mu = 1$  SLQH. However, when considering vortex excitations to be discussed in the following

$e^{i\tilde{\psi}_+^\dagger(\mathbf{x})}$  may not be single valued, therefore the fundamental angle variable is  $\tilde{\psi}_+$  instead of  $\tilde{\psi}_+ / \sqrt{2}$ .

(2) Spin-wave excitation:

While the spin sector has a neutral gapless mode. Integrating out  $\psi_+$  leads to

$$L_s = \frac{1}{2V} \frac{1}{(\mathbf{q})} \left( \frac{1}{2} \partial_t^2 \right)^2 + \frac{1}{2m} \left( \frac{1}{2} r^2 \right)^2 \quad (29)$$

where the dispersion relation of spin wave can be extracted:

$$!^2 = \left[ \frac{1}{m} V_+ (\mathbf{q}) \right] q^2 = v^2 q^2 \quad (30)$$

In the long wave-length limit:

$$V_+ (\mathbf{q}) = \frac{e^2}{d} \left( d \frac{1}{2} d^2 q + \frac{1}{6} d^3 q^2 + \dots \right); \quad qd \ll 1 \quad (31)$$

The spin wave velocity is:

$$v^2 = \frac{e^2}{m} \frac{e^2}{d} = \frac{e^2}{m} \frac{r}{2} \frac{d}{l} \quad (32)$$

Eqn 32 shows that the spin wave velocity should increase as  $1/d$  when  $d < d_c$ . At  $d = 0$ ,  $v = 0$ . This is expected, because at  $d = 0$  the  $U(1)_G$  symmetry is enlarged to  $SU(2)_G$ , the spin wave of isotropic ferromagnet  $!^2 = k^2$ . By plugging the experimental parameters  $m = 0.07m_e$  which is the band mass of GaAs,  $d = 5.2 \times 10^{-9} \text{ cm}^2$ ;  $d_l = 1.61$ ;  $r = 12.6$  into Eqn 32, we find that  $v = 1.14 \times 10^4 \text{ m/s}$ . This value is about 8 times larger than the experimental value. Although Quantum fluctuations will renormalize down the spin stiffness from  $\text{bare} = \text{to } \text{eff} < \text{bare}$ , it is known that CSGL theory can not give precise numerical values on energy gaps even in SLQH. In fact, the spin stiffness  $s$  which is defined as  $\frac{1}{2} (r^2) \frac{1}{d}$  in Eqn 29 should be determined by the interlayer Coulomb interaction instead of being dependent of the band mass  $m$ .

It is constructive to compare the spin ( $\psi_-$ ) sector of Eqn 25 with the EPQHF Hamiltonian achieved by the microscopic LLL+HF approach in [11]:

$$\begin{aligned} L = & i \frac{1}{2} \tilde{A} (\mathbf{r}) \left( \partial_t^2 + m_z (\mathbf{r})^2 \right) C q m_z (\mathbf{q}) m_z (\mathbf{q}) \\ & + \frac{A}{2} (r m_z)^2 + \frac{E}{2} [(r m_x)^2 + (r m_y)^2] \end{aligned} \quad (33)$$

where  $r_m = \frac{1}{16} \frac{A}{R_1} = m$ ,  $d = \frac{e^2 d^2}{16}$ ,  $A = \frac{e^2}{16} \int_0^1 dx x^2 \exp(-x^2/2) = \frac{e^2}{16} \frac{1}{2} \int_0^1 dx x^2 \exp(-x^2/2)$  is determined by the intralayer interaction and  $E = \frac{e^2}{16} \int_0^1 dx x^2 \exp(-x^2/2) \int_0^1 dx x^2 \exp(-x^2/2)$  is determined by the interlayer interaction. Note that all these numbers are achieved by assuming that the ground state wavefunction is Halperin's 111 wavefunction even at finite  $d$ . However as shown in [36], the wavefunction at any finite  $d$  is qualitatively different from Halperin's (111) wavefunction

which is good only at  $d = 0$ . So the numbers calculated by the LLL+HF based on (111) wavefunctions may not even have qualitatively correct distance dependence.

In the above equation, the first term is the Berry phase term, the second term is the mass (or capacitance) term, this term leads to the easy-plane anisotropy which suppresses the relative density fluctuations between the two layers, the third term is nonanalytic in the wave vector due to the long range nature of the Coulomb interaction, the fourth term is the spin stiffness term for  $m_z$  and the fifth term is the spin stiffness term for easy-plane. At  $d = 0$ ,  $m_x = C = 0$ ;  $A = E = \frac{e^2}{16\pi^2} \frac{1}{d}$ , then L in Eqn.33 reduces to the SU(2) symmetric QH ferromagnet [35] as it should be. Note that the value of  $A = E$  at  $d = 0$  is exact, because the ground state wavefunction is exactly the Halperin (111) wavefunction, while at any finite  $d$ , the estimates of  $A \neq E$  by HF approximation may be crude, because we still do not know what is the exact groundstate wavefunction which may be qualitatively different from the (111) wavefunction [11,36]. In the presence of the easy-plane ( $m_x$ ) term,  $C$  and  $A$  terms are subleading, therefore, can be dropped in the long wavelength limit. However, they are still very important if there is a instability happening at finite wavevector as shown in section III-B.

If taking the symmetry breaking direction to be along the  $x$  direction, we can write  $m_x = \frac{1}{2} m_z \cos \theta$ ;  $m_y = \frac{1}{2} m_z \sin \theta$ ;  $m_z$  with  $m_z \neq 0$ ;  $\theta \neq 0$ . Substituting the parameterization into the Berry phase term in Eqn.33, we find the Berry phase term to be  $\frac{i}{2} m_z \theta$ , if identifying  $m_z = 2$ , it is the same as the linear derivative ( $\frac{1}{2} \theta$ ) term in the spin sector of Eqn.25. However, we can see the leading term in Eqn.31 which leads to the capacitive term is  $d$ , but in Eqn.33, it is  $\frac{1}{d}$ , while the Monte-Carlo simulation in spherical geometry in [36] indicates it is  $d$ . The subleading term in Eqn.31 is non-analytic  $q$  instead of  $\frac{1}{q}$ , this is due to the long-range behavior of the Coulomb interaction. This non-analytic term is the same as that in Eqn.33 if identifying  $m_z = 2$ . The third term in Eqn.31 leads to a  $(r m_z)^2$  term with a coefficient  $\frac{1}{d^3}$ , while the coefficient of  $(r m_z)^2$  term in Eqn.33 is  $A$  which approaches the constant  $\frac{e^2}{16\pi^2} \frac{1}{d}$  as  $d \rightarrow 0$  as dictated by SU(2) symmetry at  $d = 0$ . The difficulty to recover SU(2) symmetry limit at  $d = 0$  from the CB approach is due to that the decomposition Eqn.20 in our CB approach takes advantage of the easy-plane anisotropy from the very beginning. This is similar to Abelian bosonization versus Non-Abelian bosonization in one dimensional Luttinger liquid or multi-channel Kondo model [37].

By this detailed comparison between the CB approach and the microscopic LLL+HF approach, we find that the two approaches lead to exactly the same functional form in the spin sector, some coefficients such as the Berry phase term and the non-analytic term are the same,

while some other coefficients such as the easy-plane term and spin stiffness term are not. Unfortunately, it is very difficult to incorporate the LLL projection in the CB approach. As suggested in [11], we should simply take some coefficients in CB approach as phenomenological values to be fitted into microscopic LLL+HF calculations or numerical calculations or eventually experimental data. The advantage of CB approach is that it also keeps the charge sector explicitly, therefore treat the QH effects in the charge sector and the inter-layer phase coherence in the spin sector at the same footing. While the charge sector in the LLL+HF approach is completely integrated out.

### (3) Topological excitations:

Any topological excitations are characterized by two winding numbers  $\nu_1 = 2m_1$ ;  $\nu_2 = 2m_2$ , or equivalently,  $\nu_+ = 2(m_1 + m_2) = 2m_+$ ;  $\nu_- = 2(m_1 - m_2) = 2m_-$ . It is important to realize that the two fundamental angles are  $\nu_1; \nu_2$  instead of  $\nu_+; \nu_-$ .  $m_1; m_2$  are two independent integers, while  $m_+; m_-$  are not, because  $m_+ - m_- = 2m_2$  which has to be an even integer.

There are following 4 kinds of topological excitations:  $\nu_1 = 2$ ;  $\nu_2 = 0$  or  $\nu_1 = 0$ ;  $\nu_2 = 2$ . Namely  $(m_1; m_2) = (1; 0)$  or  $(m_1; m_2) = (0; 1)$ . They correspond to inserting one flux quantum in layer 1 or 2, in the same or opposite direction as the external magnetic field. Let's classify all the topological excitations in terms of  $(q; m)$  where charge  $q$  is the fractional charge of the topological excitations in the following table.

$(m_1; m_2)$	(1;0)	(-1;0)	(0;1)	(0;-1)
$m$	1	1	1	1
$m_+$	1	1	1	1
$q$	1=2	1=2	1=2	1=2

Table 1: The fractional charge in the balanced case

The fractional charges in Table 1 were determined from the constraint  $r = a = 2$  and the finiteness of the energy in the charge sector:

$$q = \frac{1}{2} \frac{1}{a} \frac{1}{r} = \frac{1}{2} \frac{1}{2} \frac{1}{r} + \frac{1}{2} m_+ \quad (34)$$

$m = 1$  gives the vorticities which lead to logarithmic interaction between the merons, while  $q = 1=2$  lead to  $1=r$  interaction. Therefore merons are confined into the following two possible pairs at low temperature. (1) Charge neutral pairs:  $(1=2; 1)$  or  $(-1=2; 1)$ . The NGM will turn into charge neutral pairs at large wavevectors (or short distance). The pair behaves as a boson. (2) Charge 1 pair  $(1=2; 1)$  or charge -1 pair  $(-1=2; 1)$ . The pair behaves as a fermion. They are the lowest charged excitations in BLQH and the main dissipation sources for the charge transports. A duality transformation (See Eqn.43) can be easily performed to express low energy physics in terms of the dynamics of these topological excitations. There is a possible Kosterlitz-Thouless

(KT) transition above which the meron pairs are liberated into free meron.

The MCF picture in the last section points to two interesting possibilities (1) There maybe Charge neutral bosonic excitations with  $(0; 1)$ : Note that  $m_+ = 0$  implies  $m_1 = m_2 = m$  and  $m = 2m$ . For  $m = 1$ , it corresponds to inserting one ux quantum in layer 1 in one direction and one ux quantum in layer 2 in the opposite direction. So only  $(0; 2)$  exist, while  $(0; 1)$  do not exist. (2) There may be deconfined (or free)  $1=2$  charged excitations. Because any excitations with non-vanishing  $m$  will be confined, so any deconfined excitations must have  $m = 0$  which implies  $m_1 = m_2 = m$  and  $m_+ = 2m$ . We find the charge  $q = \frac{1}{2}m_+ = m$  must be an integer. This proof rigorously rules out the possibility of the existence of deconfined fractional charges. We conclude that any deconfined charge must be an integral charge.  $m_1 = m_2 = 1$  corresponds to inserting one ux quantum through both layers which is conventional charge 1 excitation. Splitting the two uxes will turn into a meron pair with the same charge.

Most of the results achieved in this subsection were achieved before [10,11,2] in microscopic calculations. In these calculations, the charge fluctuations were integrated out, the LLL projections were explicitly performed and HF approximations were made. Here, we reproduce these old results in a very simple way which keeps both spin and charge in the same footing and bring out the spin-charge connection in a very transparent way. We also classify all the possible excitations in this effective CB approach.

In the next section, I will study a completely new state which may be the real ground state directly relevant to the experiments.

#### B. Balanced case $m_1 = m_2 = 1=2$ : Inhomogeneous excitonic super uid state

The discussions in the last section are in the homogeneous exciton super uid state, now we will study the instability of this ESF state as the distance is increased. As stated in the introduction, when the distance is smaller than  $d_{c1}$ , the system is in the ESF state, while it is sufficiently large, the system becomes two weakly coupled  $1=2$  Composite Fermion Fermi Liquid (FL) state. There could be a direct first order transition between the two states. However, the experimental observations that both zero voltage tunneling peak [4] and the Hall drag resistivity [5] develop very gradually when  $d > d_2$  suggest the transition at  $d = d_{c2}$  is a 2nd order phase transition. Although there are very little dissipations in both the ESF and FL, the experiment [41] discovered strong enhancement of drag and dissipations in an intermediate distance regime. These experimental observations suggest that there must be intermediate phases between the

two phases. As shown in this section, the intermediate phase could be inhomogeneous excitonic super uid (I-ESF) (Fig 3). In the following, we will apply the quantum Ginzburg-Landau theory developed in [22] to study the most likely phase diagram of 2d BLQH system as the distance increases. We assume that Eqn 23 and its dual action work on both sides until  $d = d_{c2}$  beyond which the I-ESF melts into two weakly coupled FL state (Fig 3).

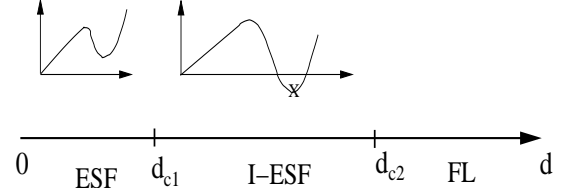


Fig 3: The zero temperature phase diagram in the balanced case as the distance between the two layers increases. ESF stands for excitonic super uid, I-ESF stands for inhomogeneous excitonic super uid, FL stands for Fermi Liquid. Energy dispersion relations in these phases are also shown. The cross in the I-ESF means the negative magneto-roton minimum is replaced by density wave formation in the pseudo-spin sector [38].

In order to study the instability of the ESF to the formation of I-ESF, one need to extend the dispersion relation Eqn.30 to include higher orders of momentum:

$$\epsilon^2 = q^2 (a - bq + cq^2) \quad (35)$$

where  $a, b, c > 0$  and as explained in the last subsection, the non-analytic term due to the long-range Coulomb interaction survives the LLL projection.

As shown in [22], the advantage to extend the dispersion relation beyond the leading order is that the GL action can even capture possible phase transitions between competing orders due to competing interactions on microscopic length scales.

As explained in the last section, in the LLL-HF approach in [11], these coefficients were found to be  $a = d^2; b = d^2$ , but  $c$  remains a constant at small distances. It can be shown that the dispersion curve Eqn.35 indeed has the shape shown in Fig.3. When  $b = d^2 < b_c = 2^2 \frac{p}{ac}$ , the magneto-roton minimum has a gap at  $q = q_0 = \frac{p}{a-c}d$ , the system is in the ESF state, this is always the case when the distance  $d$  is sufficiently small. However, when  $b = b_c$ , the magneto-roton minimum collapses at  $q = q_0$  which signifies the instability of the ESF to a density wave formation as shown in [22]. When  $b = d^2 > b_c = 2^2 \frac{p}{ac}d$ , the minimum drops to negative and is replaced by a stable density wave formation, the system gets to the I-ESF state, this is always the case when the distance  $d$  is sufficiently large. The phenomenon of the collapsing of the magneto-roton minimum as the distance increases was also seen in the numerical calculations in the LLL+HF approaches [11,45]. It was estimated that  $q_0 \ll 1$ , so the lattice constant of

the DW is of the same order of magnetic length  $l$  which is  $10\text{\AA}$ . The critical distance  $d_{c1}$  is also of the same order of the magnetic length. It is very interesting to see if soft X-ray or light scattering experiments [49] can directly test the existence of the DW when  $d_{c1} < d < d_{c2}$ .

It may be necessary to point out the difference between single layer QH and bilayer QH. In the SLQH, there is no true symmetry breaking, the Goldstone mode at  $k = 0$  is absent due to the Higgs mechanism. In fact,  $k = 0$  turns out to be a local maximum. There is still a magnetoroton minimum at  $q_0 \sim 1$ , the collapsing of the minimum also signifies the collapsing of the QH gap, the system gets to a possible Wigner crystal state. In the BLQH, the pseudo-spin sector is a charge neutral sector, as shown in [22], both low energy modes at  $k = 0$  and  $k = k_0$  are important. The collapsing of the minimum in the charge neutral sector does not signify the collapsing of the QH gap in the charge sector, so the system remains in QH state. This is also one of reasons why the BLQH shows many interesting phenomena not displayed in SLQH.

In the IESF, the exciton pairing amplitude becomes  $\Psi = ae^{i\phi_1} + e^{i\phi_2} \sum_{m=1}^P e^{iQ_m \cdot \mathbf{x}}$ . As pointed out in [22], the possible lattice structures of the DW depend on many microscopic details. It is known that for a bosonic system, up to a global phase, the ground state wavefunction has to be real and positive, so  $\phi_1 = \phi_2$  can be set to be zero,  $Q_m$  have to be paired as anti-nodal points, so  $P$  has to be even. The point group symmetry of the lattice dictates  $\sum_{m=1}^P e^{iQ_m \cdot \mathbf{x}}$  to be real. These constraints lead to  $\Psi = e^{i\phi} (a + 2 \sum_{m=1}^{P/2} \cos Q_m \cdot \mathbf{x})$  where  $\phi = a/P$  to keep  $\Psi$  to be free of nodes. In principle, higher Fourier components may also exist, but they decay very rapidly, so can be neglected without affecting the DW structure qualitatively. In two dimension, the most common lattices are 1d stripe embedded in two dimension, square and hexagonal lattices shown in Fig. 4 (a) and (b) and (c) respectively. In the following, I will discuss stripe, square and hexagonal lattices respectively.

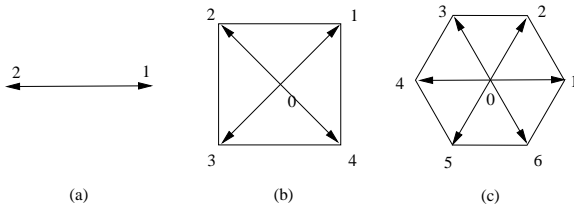


Fig 4: (a) 2 shortest reciprocal lattice vectors in a stripe (b) 4 shortest reciprocal lattice vectors in square lattice. (c) 6 shortest reciprocal lattice vectors in hexagonal lattice.

(a)  $P=2$ :  $Q_1 = -Q_2 = Q$  are a pair of anti-nodal points (Fig. 4a). They are the two shortest reciprocal lattice vectors generating a 1 dimensional lattice embedded in a 2 dimensional system. The field is  $\Psi(\mathbf{x}) = a + 2 \cos Q \cdot \mathbf{x}$ . The local density wave operator  $\frac{1}{D_W} = j(\mathbf{x})^2 = (a + 2 \cos Q \cdot \mathbf{x})^2$ . It breaks

translational invariance only along 1-dimension which is similar to Smectic-A or Smectic-C phase in the liquid crystal [42]. The maxima of the DW  $m_{\text{ax}} = a + 2$  form a stripe, while the minima  $m_{\text{in}} = a - 2 > 0$  appear exactly in the middle of stripe at  $\mathbf{a} = \frac{1}{2}\mathbf{a}_1$ . They form the dual lattice of the maxima stripe which is also a stripe.

(b)  $P=4$ :  $Q_3 = -Q_1, Q_4 = -Q_2, Q_1 \cdot Q_2 = 0$ ,  $Q_i, i=1;2;3;4$  form the 4 corners of a square (Fig. 4b). They are the four shortest reciprocal lattice vectors generating a 2 dimensional square lattice. The pairing field is  $\Psi(\mathbf{x}) = a + 2 (\cos Q_1 \cdot \mathbf{x} + \cos Q_2 \cdot \mathbf{x})$ . The local density wave operator  $\frac{1}{D_W} = j(\mathbf{x})^2$ . The maxima of the DW  $m_{\text{ax}} = a + 4$  form a 2d square lattice, while the minima of the DW  $m_{\text{in}} = a - 4 > 0$  appear exactly in the middle of lattice points at  $\mathbf{a} = \frac{1}{2}(\mathbf{a}_1 + \mathbf{a}_2)$ . They form the dual lattice of the maxima square lattice which is also a square lattice.

(c)  $P=6$ .  $Q_i, i=1;2;3;4;5;6$  form the 6 corners of a hexagon (Fig. 4c). They consist of the 6 shortest reciprocal lattice vectors generating a 2 dimensional hexagonal lattice. The pairing field is  $\Psi(\mathbf{x}) = a + 2 (\cos Q_1 \cdot \mathbf{x} + \cos Q_2 \cdot \mathbf{x} + \cos Q_3 \cdot \mathbf{x})$ . The local density wave operator  $\frac{1}{D_W} = j(\mathbf{x})^2$ . The maxima of the DW  $m_{\text{ax}} = a + 6$  form a 2d hexagonal lattice. While the minima of the DW  $m_{\text{in}} = a - 6 > 0$  appear in the middle of lattice points at  $\mathbf{a} = \frac{1}{3}(\mathbf{a}_1 + \mathbf{a}_2)$ . They form the dual lattice of the maxima hexagonal lattice which is a honeycomb lattice.

Because the IESF breaks both global U(1) rotation symmetry and translational symmetry, there are three Goldstone bosons: one superfluid phonon mode and two lattice phonons in 2 dimension. The ODLRO is characterized by  $\Psi = e^{i\phi}$ , the translational order is characterized by  $Q_m = e^{iQ_m \cdot \mathbf{r}}$ , the orientational order is characterized by  $\phi_{\text{or}} = e^{i6\phi}$  for the hexagonal lattice and  $\phi_{\text{or}} = e^{i4\phi}$  for the square lattice where  $\phi = \frac{1}{2}\mathbf{r} \cdot \mathbf{u}$ . For the 1d stripe, there is only one lattice phonon. The 1d stripe will lead to transport anisotropy which was not seen in experiments, so will not be considered any more in the following.

It is known that at any finite temperature at  $d = 2$ , there is no true long range order except possible long-range orientational order [40]. We can apply the Kosterlitz-Thouless-Halperin-Nelson-Young (KTHNY) theory [40] to the phases in Fig. 3. When interlayer distance  $d = 0$ , the symmetry is SU(2), the broken symmetry state at  $T = 0$  in Fig. 3 is immediately destroyed at any finite  $T$  in Fig. 5. The system becomes the exciton liquid (EL). When  $0 < d < d_{c1}$ , the true long-range ordered ESF in Fig. 3 has only algebraic ODLRO in Fig. 5, there is a finite temperature  $KT$  transition above which the system is in the EL. When  $d_{c1} < d < d_{c2}$ , the true long-range ordered IESF in Fig. 3 has only algebraic ODLRO and translational order, but true orientational

order. There is a finite temperature  $KT$  transition characterized by the exciton operator  $\psi = e^i$ . Due to the formation of the DW, there is a discontinuous drop in  $T_{KT}$  across  $d = d_{c1}$ . There could also be a dislocation driven transition at  $T = T_v$  in the universality class of 2d vector Coulomb gas with the correlation length exponent  $\nu = 0.37$ . The system is in the exciton hexatic density wave (EHDW) phase with short range translational order and algebraic orientational order. There could also be a disclination driven transition at  $T = T_s$  in the universality class of  $KT$  transition (scalar Coulomb gas) with the correlation length exponent  $\nu_s = 1/2$ . The system becomes exciton liquid phase.

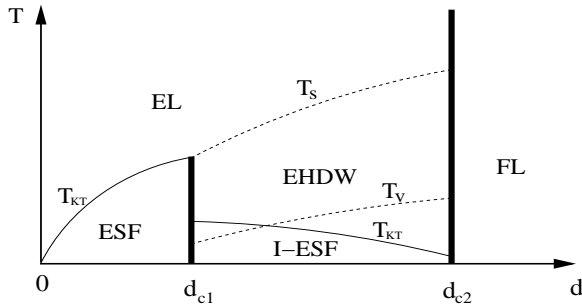


Fig 5: The Finite temperature phase diagram in the balanced case as the distance between the two layers increases. ESF stands for excitonic superfluid with only algebraic OD LRO. I-ESF stands for inhomogeneous excitonic superfluid with only algebraic OD LRO, algebraic translational order and true orientational order. The EHDW stands for the exciton hexatic density wave phase with only algebraic orientational order. FL stands for Fermi liquid.  $T_{KT}$  is the  $KT$  transition temperature driven by vortex unbinding in the phase. The dashed  $T_v$  line is the vector Coulomb gas transition temperature driven by dislocation unbinding. The dashed  $T_s$  line is the scalar Coulomb gas transition temperature driven by disclination unbinding. The thick lines are 1st order transitions, while thin and dashed lines are 2nd order transitions.

Inside the I-ESF, as the distance increases,  $a$  decreases, so  $T_{KT}$  drops, while  $\nu$  increases, so  $T_v$  and  $T_s$  also increases as shown in the Fig.5. When  $d \rightarrow d_{c2}$ ,  $a \rightarrow P$ . At the minimum lattice points  $m_{in} = a/P$ , the exciton pairings almost vanish. When the minimum pairings finally vanish at  $d = d_{c2}$  where  $a = P$ , the excitons break up to two Composite Fermion in two separate layers. There is a 1st order transition at  $d = d_{c2}$  to the weakly coupled CF state as shown in Fig.3. The flux attachment transformation Eqn.18 which treats the electrons in the two layers on the same footing breaks down and a completely different flux attachment transformation within a single layer to transform an electron into a Composite Fermion Eqn.5 must be used [30]. Unfortunately, because completely different actions are needed in the two sides of the transition at  $d = d_{c2}$ , this quantum phase transition can not be addressed in this paper and remains an interesting open question. At  $d < d_{c2}$ ,

it is the composite boson to feel zero field, they are condensed into either the ESF or the I-ESF states, while at  $d > d_{c2}$ , it is the composite fermion to feel zero field, they form a Fermi surface. As explained in the introduction, the zero temperature phase diagram Fig.3 resembles the superconductor in a Zeeman field with the Zeeman splitting corresponding to the layer distance. The superconductor becomes the inhomogeneous LOFF state first before turning into a normal Fermi liquid state.

The I-ESF state has many interesting properties. The meron excitations characterized in the Table 1 still hold in the I-ESF state. The charge sector remains gapped, the system is still in the QH state. As shown in [22], the superfluid density of I-ESF is much smaller than that of ESF, a single meron has a much larger core size than that in the ESF. The two factors lead to much smaller excitation energy of a single meron, therefore much smaller critical velocity in the I-ESF. The precise energy of a single meron in the I-ESF will be investigated in a separate publication [39]. Due to its very low critical velocity, it is possible that the driving current in the counter-flow experiment [6] already exceeded the critical current to cause the large dissipation observed in the experiments. Or the temperature is already above the  $T_{KT}$  in the I-ESF. If this is the case, the I-ESF resolves the outstanding problem where the dissipations come from in the interlayer tunneling and counter-flow experiments which directly probe the pseudo-spin channel. Because the I-ESF differs from the ESF only in the pseudo-spin sector, the charge sector in both states is more or less the same, so the Coulomb drag and Hall drag experiments which show the QH effect in the charge sector is the same.

It was also argued [12,6] that the disorder may play important roles even inside the ESF phase. We expect it is even more important inside the I-ESF phase due to its small superfluid density and DW structure. The disorder may also smear the two first order transitions at  $d_{c1}$  and  $d_{c2}$  into a two 2nd order transitions. The disorder may also transfer the long range DW orders into short range ones. The fact make the observation of the DW structure by light scattering difficult.

In the next two subsections, we will study the effects of the imbalance.

#### C. Im-balanced case $\mu_1 \neq \mu_2$ : excitonic superfluid state

##### (1) 0-diagonal algebraic order and Spin-wave excitation:

In the im-balanced case, the second term in Eqn.23 includes the coupling between spin sector and charge sector even when neglecting vortex excitations. Expanding this term, we find the effective action of the coupled  $+$  and  $-$  modes:

$$\begin{aligned}
L_c = & \frac{1}{8} + (\mathbf{q}; !)_- \left[ \frac{!^2 + !_q^2}{V_+ (\mathbf{q}) + \frac{4}{m} \frac{1}{q^2}} \right] + (\mathbf{q}; !)_+ \\
& + \frac{1}{8} (\mathbf{q}; !)_- \left[ \frac{!^2}{V_+ (\mathbf{q})} + \frac{1}{m} q^2 \right] (\mathbf{q}; !)_+ \\
& + \frac{1}{4m} (1_+ 2_-) q^2 (\mathbf{q}; !)_+ (\mathbf{q}; !)_- \quad (36)
\end{aligned}$$

where we safely dropped a linear derivative term in Eqn. 23 in the Interlayer Coherent QH state. However, the linear derivative term will be shown to play important role in the incoherent disordered state in the next subsection. From Eqn.36, we can identify the three propagators:

$$\begin{aligned}
\langle + + \rangle &= \frac{(\frac{4m}{q^2}) (!^2 + v^2 q^2) !_q^2}{!^4 + !^2 (!_q^2 + v^2 q^2) + f v^2 q^2 !_q^2} \\
\langle - - \rangle &= \frac{4V_+ (\mathbf{q}) (!^2 + !_q^2)}{!^4 + !^2 (!_q^2 + v^2 q^2) + f v^2 q^2 !_q^2} \\
\langle + - \rangle &= \frac{4(1_+ 2_-) V_+ (\mathbf{q}) !_q^2}{!^4 + !^2 (!_q^2 + v^2 q^2) + f v^2 q^2 !_q^2} \quad (37)
\end{aligned}$$

where  $f = 4(1_+ 2_-) !_q^2 = !_c^2 + \frac{1}{m} q^2 V_+ (\mathbf{q})$ , the cyclotron frequency  $!_c = \frac{2}{m}$  and the spin wave velocity in the balanced case  $v^2 = \frac{1}{m} V_+ (\mathbf{q})$  were defined in Eqn.32.

Performing the frequency integral of the first equation in Eqn.37 carefully, we find the leading term of the equal time correlator of  $+$  stays the same as the balanced case Eqn.27:

$$\langle + (\mathbf{q}) + (\mathbf{q}) \rangle = 2 \frac{2}{q^2} + O\left(\frac{1}{q}\right) \quad (38)$$

which leads to the same algebraic order exponent 2 as in the balanced case Eqn.28.

We conclude that the algebraic order in the charge sector is independent of the imbalance. This may be expected, because the total filling factor  $\nu = 1$  stays the same.

In the  $q; ! \rightarrow 0$  limit, we can extract the leading terms of the propagator:

$$\langle - - \rangle = \frac{4V_+ (\mathbf{q})}{!^2 + f v^2 q^2} \quad (39)$$

where we can identify the spin wave velocity in the imbalanced case:

$$v_{im}^2 = f v^2 = 4(1_+ 2_-) v^2 = 4(1_+ 1_-) v^2 \quad (40)$$

which shows that the spin-wave velocity attains its maximum at the balanced case and decreases parabolically as the imbalance increases. The corresponding  $K T$  transition temperature  $T_{KT}$  also decreases parabolically as the imbalance increases.

Similarly, in the  $q; ! \rightarrow 0$  limit, we can extract the leading terms in the  $+$  propagator:

$$\langle + - \rangle = \frac{4V_+ (\mathbf{q}) (1_+ 2_-)}{!^2 + f v^2 q^2} = (1_+ 2_-) \langle - - \rangle \quad (41)$$

which shows that the behavior of  $\langle + - \rangle$  is dictated by that of  $\langle - - \rangle$  instead of  $\langle + + \rangle$ .

When the vortex excitations to be discussed in the following are included, the spin wave velocity will be renormalized down. As analyzed in detail in the last subsection, it is hard to incorporate the Lowest Landau Level (LLL) projection in the CB approach, so the spin wave velocity can only taken as a phenomenological parameter to be fitted to the microscopic LLL calculations or experiments. But we expect that the forms of all the propagators stay the same.

## (2) Topological excitations

There are following 4 kinds of topological excitations:

$1_- = 2_-$ ;  $2_- = 0$  or  $1_- = 0$ ;  $2_- = 2_-$ . Namely  $(m_1; m_2) = (1; 0)$  or  $(m_1; m_2) = (0; 1)$ . We can classify all the possible topological excitations in terms of  $(q; m_-)$  in the following table.

$(m_1; m_2)$	$(1; 0)$	$(-1; 0)$	$(0; 1)$	$(0; -1)$
$m_-$	1	1	1	1
$m_+$	1	1	1	1
$q$	1	1	2	2

Table 2: The fractional charge in imbalanced case

The fractional charges in table 2 were determined from the constraint  $\nu = 2$  and the finiteness of the energy in the charge sector:

$$\begin{aligned}
q &= \frac{1}{2} \int d\mathbf{r} \left[ \mathbf{r} \cdot \nabla \times \mathbf{r} + (1_+ 2_-) \mathbf{r} \cdot \nabla \right] \mathbf{r} \\
&= \frac{1}{2} [m_+ + (1_+ 2_-) m_-] \quad (42)
\end{aligned}$$

In contrast to the balanced case where  $q$  only depends on  $m_+$ ,  $q$  depends on  $m_+$ ;  $m_-$  and the filling factors  $1_+$ ;  $2_-$ . Just like in balance case, any deconfined excitations with  $(m_- = 0; m_+ = 2m_-)$  have charges  $q = \frac{1}{2} m_+ = m_-$  which must be integers. While the charge of  $(m_+ = 0; m_- = 2m_-)$  is  $q = (1_+ 2_-) m_-$  which is charge neutral only at the balanced case.

The merons listed in table 2 are confined into the following two possible pairs at low temperature. (1) Charge neutral pairs:  $(1_+; 1_-)$  or  $(2_-; 1_-)$ . They behave as bosons. The NGM will turn into charge neutral pairs at large wavevectors. (2) Charge 1 pair  $(1_+; 1_-) + (2_-; 1_-)$  or charge -1 pair  $(-1_+; 1_-) + (-2_-; 1_-)$ . They behave as fermions. They are the lowest charged excitations in BLQH and the main dissipation sources for the charge transports.

## (3) Dual action

A duality transformation can be easily performed to express low energy physics in terms of the dynamics

of these topological excitations. Performing the duality transformation on Eqn.23 leads to the dual action in terms of the vortex degree of freedom  $J^v = \frac{1}{2} \theta \theta = J^{v1} J^{v2}$  and the corresponding dual gauge fields  $b$ :

$$\begin{aligned} L_d = & i \dot{b} \theta - b^+ i A_s^+ \theta - b^+ + i b^+ J^{v+} \\ & + \frac{m}{2f} (\theta b_0^+ - \theta b^+)^2 + \frac{1}{2} (r - \tilde{b}^+) V_+ (\theta) (r - \tilde{b}^+) \\ & i A_s \theta - b + i b J^v - h_z (r - \tilde{b}) \\ & + \frac{m}{2f} (\theta b_0 - \theta b)^2 + \frac{1}{2} (r - \tilde{b}) V_- (\theta) (r - \tilde{b}) \\ & - \frac{m}{f} (\theta_1 - \theta_2) (\theta b_0 - \theta b) (\theta b_0^+ - \theta b^+) \end{aligned} \quad (43)$$

where  $A_s = A_s^1 - A_s^2$  are the two source fields. The last term can be shown to be irrelevant in the ILCH state. The spin wave velocity in Eqn.40 can also be easily extracted from this dual action. Note that the spin (or  $\theta$ ) sector of this dual action takes similar form as a 3D superconductor in an external magnetic field  $h_z$ .

It is constructive to compare this dual action derived from the CB approach with the action derived from MCF approach Eqn.8. We find the following three differences: (1) The topological vortex degree of freedom  $J^v$  are missing in Eqn.8. These vortex degree of freedom are needed to make the variable  $\theta$  in Eqn.10 to be an angle variable  $0 < \theta < 2\pi$ . (2) The  $\theta$  terms in Eqn.8 are extra spurious terms. These extra spurious terms break SU(2) symmetry even in the dilute limit. (3) The linear term  $h_z (r - \tilde{b})$  is missing in Eqn.8. This linear term is not important in the interlayer coherent QH state, but it is very important in the incoherent disordered state to be discussed in the following subsection. Indeed, if we drop all the  $\theta$  terms, use bare mass and also add the topological vortex currents and the linear term by hands in Eqn.8, then Eqn.8 will be identical to Eqn. 43. We conclude that Eqn. 23 and 43 from CB approach are the correct and complete effective actions.

We can also look at the static energy of a charge 1 meron pair consisting a meron with charge  $q_1$  and charge  $q_2$  separated by a distance  $R$ :

$$E_{mp} = E_{1c} + E_{2c} + \frac{1}{2} \frac{e^2}{R} + 8 \frac{1}{2} s_0 \ln \frac{R}{R_c} \quad (44)$$

where  $E_{1c}, E_{2c}$  are the core energies of meron 1 (charge  $q_1$ ) and meron 2 (charge  $q_2$ ) respectively,  $R_c$  is the core size of an isolated meron,  $s_0 = \frac{1}{8m}$  is the spin stiffness at the balanced case.

Minimizing  $E_{mp}$  with respect to  $R$  leads to an optimal separation:  $R_o = \frac{e^2}{8 s_0}$  which, remarkably, is independent of the imbalance. Namely, the optimal separation of a meron pair remains the same as one tunes the imbalance. Plugging  $R_o$  into Eqn.44 leads to the optimal energy of a meron pair:

$$E_o = E_{1c} + E_{2c} + \frac{1}{2} \left( \frac{e^2}{R_o} + 8 s_0 \ln \frac{R_o}{R_c} \right) \quad (45)$$

Because of logarithmic dependence on  $R_c$ , we can neglect the  $1/R_c$  dependence in  $R_o$ , then the second term in Eqn.45 decreases parabolically as imbalance increases. Unfortunately, it is hard to know the  $1/R_c$  dependence of  $E_{1c}, E_{2c}$  and  $R_c$  from an effective theory, so the dependence of the energy gap  $E_o$  on  $1$  is still unknown.

#### D. Imbalanced case $1 \neq 2$ : Inhomogeneous excitonic superfluid state

In ESF state, there is a QH charge gap in the charge sector but gapless in the spin sector. As shown in III-B, in the I-ESF phase, the spin sector remains gapless and has additional gapless lattice phonon modes, but the charge sector remains gapped. So we can integrate out the gapped charge sector and focus on the effective action in the spin sector [43]:

$$L_s = \frac{i}{2} \theta \dot{\theta} + \frac{f}{2m} \left( \frac{1}{2} r \right)^2 + \frac{1}{2} V_-(\theta) - h_z \quad (46)$$

where the imbalance field  $h_z$  couples to the conserved quantity  $\theta$ .

Integrating out  $\theta$  leads to

$$L_h = \frac{1}{2V_-(\theta)} \left( \frac{1}{2} \dot{\theta} + i h_z \right)^2 + \frac{f}{2m} \left( \frac{1}{2} r \right)^2 \quad (47)$$

where  $h_z = V_-(\theta_1 - \theta_2)$  plays the role of the time component of imaginary gauge field.

Setting the exciton operator  $\psi = e^{i\theta}$ , the above "hard" spin model becomes a "soft" spin model:

$$\begin{aligned} L_s = & h_z (\psi; ) \psi (x; ) + j \psi (x; )^2 + j^* \psi (x; )^2 \\ & + j \psi (x; )^2 + u j \psi (x; )^2 + \end{aligned} \quad (48)$$

Obviously, the imbalance  $h_z$  term breaks the  $Z_2$  symmetry which corresponds to the P-H symmetry  $\psi \rightarrow \psi^*$ . In the ESF phase  $\langle \psi \rangle = a$ , in the I-ESF phase,  $\langle \psi \rangle = a + 2 \sum_{m=1}^P \cos Q_m x$  where  $a = P$ . In both phases,  $\psi (x; ) \psi (x; ) = 0$  at mean field level, so the  $h_z$  is irrelevant. However, it may play an important role in the FL phase in Fig. 3.

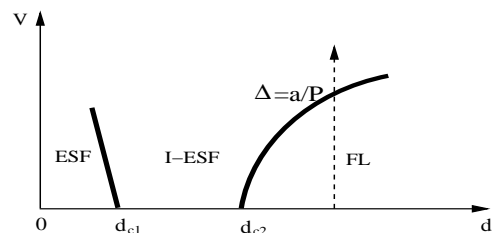


Fig 6: The bias voltage  $V$  versus distance  $d$  phase diagram of model Eqn.23 at zero temperature. Thick (thin) line is a 1st (2nd) order transition. The dashed line is the bias voltage induced FL to I-E SF transition investigated in the experiment [47]

In order to see how the imbalance affects the shape of the dispersion curve shown in the Fig.3, we need to push Eqn.39 to the order  $q^4$ :

$$\epsilon_{\text{imb}}^2 = f \epsilon_b^2 - f(1 - f) \frac{v^4 q^4}{\epsilon_c^2} \quad (49)$$

where  $\epsilon_b^2$  is defined in Eqn.35.

Scaling out the common factor  $f$ , one can see  $a$  and  $b$  stay the same, while  $c$  is reduced by the imbalance. Therefore  $q_b$  increases, namely, the wavelength of the DW is reduced. While  $b_c$  decreases, namely, the critical distance  $d_{c1}$  also decreases. This is why the first order transition line at  $d_{c1}$  in Fig. 6 bends to the left slightly as  $V$  increases.

As shown in III-B, when the distance of the two layers is further increased to larger than a second critical distance  $d_{c2}$  where  $\epsilon = a=P$  and the minimum pairings in the I-E SF finally vanish, the excitons break up to two Composite Fermion in two separate layers. There is a 1st order transition to the CF state as shown in Fig.3. The effective action Eqn.48 is not valid any more beyond  $d_{c2}$ . However, it can still be applied to approach the I-E SF to FL transition line where  $\epsilon = a=P$  from the left in Fig. 6. The detailed shape of this boundary is hard to achieve, but we can draw some analogy from the results achieved in [62] and sketch it in Fig.6. The dashed line in Fig.6 was investigated in recent experiment [47], a parabolic behavior  $h_z^2 \propto d - d_1$  was found for the shape of the transition at very small imbalances.

Fig. 6 is valid only for small imbalance such that  $\nu_1, \nu_2$  do not fall onto any fractional Quantum Hall plateaus for separate layers. For large imbalance such as two layers with  $\nu_1 = 1/3; \nu_2 = 2/3$  still with  $\nu_T = 1$ , then the two weakly coupled layers show  $\nu_1 = 1/3$  and  $\nu_2 = 2/3$  fractional Quantum Hall states separately when  $d > d_{c2}$ . Because there are intralayer gaps, they are more robust against the interlayer correlations, we expect  $d_{c2}$  for  $\nu_1 = 1/3; \nu_2 = 2/3$  to be smaller than  $\nu_1 = \nu_2 = 1/2$ . If we bring them closer, there could be a direct 1st order transition at  $d_{c1} = d_{c2}$  from the weakly coupled pair to the E SF, or through a narrow regime of I-E SF.

#### E. Interlayer tunneling

Note that in contrast to MCF, the same phase factor appears in the singular gauge transformation Eqn.18 for the two layers  $a = 1/2$  which get canceled exactly in  $H_t$ :

$$\begin{aligned} H_t &= t \frac{v}{\epsilon} (\mathbf{x})_2 (\mathbf{x}) + h \mathbf{x} \cdot \mathbf{z} = 2t \frac{v}{\epsilon} \cos(\theta_1 - \theta_2) \\ &= 2t \frac{v}{\epsilon} \cos \end{aligned} \quad (50)$$

where the exciton operator is  $C_1^\dagger C_2 = \frac{v}{\epsilon} \frac{1}{2} e^{i\theta_1 - \theta_2}$ .

In the presence of in-plane magnetic field  $B_{jj} = (B_x, B_y)$ , the effective Lagrangian is:

$$\begin{aligned} L_s &= \frac{1}{2V} \frac{1}{\epsilon} \left( \frac{1}{2} \partial_t + i h_z \right)^2 + \frac{1}{2m} (\mathbf{r} \cdot \nabla)^2 \\ &+ 2t \frac{v}{\epsilon} \cos(\mathbf{Q} \cdot \mathbf{x}) \end{aligned} \quad (51)$$

where  $\mathbf{x} = (x, y); \mathbf{Q} = \left( \frac{2\pi B_y}{\phi_0}; \frac{2\pi B_x}{\phi_0} \right)$ .

In balanced case, it was found that when the applied in-plane magnetic field is larger than a critical field  $B > B_{jj} = (\epsilon = s_0)^{1/2}$ , there is a phase transition from a commensurate state to an incommensurate state with broken translational symmetry. When  $B > B_{jj}$ , there is a finite temperature  $KT$  transition which restores the translation symmetry by means of dislocations in the domain wall structure in the incommensurate phase.

As can be seen from Eqn.51,  $s = \frac{1}{2}$ , while  $t \propto \frac{1}{\epsilon^{1/2}}$ , so the critical field  $B_{jj} = (\epsilon = s)^{1/2} = \frac{1}{2}$  increases as one tunes the imbalance.

How these results achieved in the E SF phase change in the I-E SF phase will be investigated in [39].

#### F. Comparison with earlier work

In this section, I assumed that for balanced BLQH, there are two critical distances  $d_{c1} < d_{c2}$ . When  $0 < d < d_{c1}$ , the system is in the exciton superfluid (ESF), when  $d_{c1} < d < d_{c2}$ , the system is in the inhomogeneous exciton superfluid (I-E SF) phase, there is a 1st order transition at  $d_{c1}$  driven by the collapsing of magneto-roton minimum. When  $d_{c2} < d < 1$ , the system becomes two weakly coupled  $\nu_1 = 1/2$  Composite Fermion FL (CFFL) state. There is also a first order transition at  $d = d_{c2}$ . From this picture, when  $d > d_{c2}$ , applying bias voltage across the two layers may drive the system from the FL into the I-E SF state.

Although the ESF phase and FL phase at the two extreme distances are well established, the picture of how the ESF phase evolves into the two weakly-coupled FL states is still not clear, namely, the nature of the intermediate phase at  $d_{c1} < d < d_{c2}$  is still under debate. There are other proposals except the one proposed in this paper. By the microscopic LLL+ HF approach, the authors in [44-46] claimed that the transition at  $d_{c1}$  is an instability to a pseudospin density wave state driven by the gap closing of magneto-roton minimum at a finite wave-vector. Their results showed that on the ordered side, the imbalance increases the spin stiffness, on the disordered side, the imbalance drives a quantum phase transition from the pseudospin density wave state to the ESF. The properties of this pseudo-spin density wave are not addressed in [44-46]. In this paper, we argued that



this pseudo-spin density wave state is just the I-E SF state which is still a QH state in the charge sector, but inhomogeneous exciton pairing in the pseudo-spin sector. We also argued that this I-E SF may be the true ground state responsible for all the experimental facts.

As stated in the previous sections, the advantage of this microscopic LLL+HF approach over the CB approach used in this paper is that the calculations were performed explicitly in the LLL. However, all the calculations in LLL+HF approach assumes that the ground state wavefunction at any finite  $d$  is still the (111) wavefunction. As shown in [36], the wavefunction at any finite  $d$  is qualitatively different from the (111) wavefunction which is good only at  $d = 0$ . So the excitation spectra calculated by the LLL+HF based on the (111) wavefunction may not even have qualitatively correct distance dependence. The CB field theory approach in this paper circumvents this difficulty associated with the unknown wavefunction at any finite  $d$ . Furthermore, in this LLL+HF approach, the charge fluctuations are completely integrated out, therefore can not address the interplay between the QH effects in the charge sector and the interlayer phase coherence in the spin sector. It was shown in section B that in the in-balanced BLQH, there is a coupling between the charge sector and the spin sector even when ignoring all the topological excitations. This coupling renormalizes down the spin-wave velocity. As stated in section C, the charge sector also becomes gapless at  $d_{c1}$ , so its fluctuation can not be ignored near  $d_{c1}$ . However, as pointed out in the introduction and section A, it is hard to incorporate the LLL projection. Some parameters can only be estimated in the LLL+HF approaches. So the CB approach in this paper and the microscopic LLL+HF approach in [45] are complementary to each other. Recently, a trial wavefunction involving the coexistence of composite bosons and composite fermions at finite distance was proposed in [50]. However, it seems to the author that there is no phase transitions in this CF-CB coexistence trial wavefunction. The authors in [51] argued that the state  $d_{c1} < d < d_{c2}$  is a phase separated state between the ESF and the FL. Based on this phase separation picture, Wang investigated the effect of the interlayer tunneling [52].

#### IV. CONCLUSIONS

Three common approaches to SLQH systems are the wavefunction (or first quantization) [48,28], Composite Fermion Field Theory (CFFT) [29,31] and Composite Boson Field Theory (CBFT) approaches [33,34]. The Composite Fermion Wavefunction (CFW) [28] approach has been quite successfully applied to study SLQH at Jain's series at  $\nu = \frac{p}{2sp+1}$ . CFFT has been successfully used to study the CF Fermi liquid at  $\nu = 1/2$  which is at the end point of Jain's series in the limit  $p \rightarrow 1$ .

However, there are some problems with CFFT approach whose equivalence to the CFW is still not obvious even in SLQH. These problems have been vigorously addressed in [31]. CBFT approach has so far only limited to Laughlin's series  $\nu = \frac{1}{2s+1}$  which is only a  $p = 1$  subset of Jain's series. It can not be used in any simple way to study  $p > 1$  Jain series and  $\nu = 1/2$  CF Fermi liquid. But it has also been applied successfully in  $\nu = 1$  spin-unpolarized QH systems [35]. In this paper, we used both CFFT and CBFT approach to study the balanced and in-balanced BLQH systems. We found that CBFT approach is superior than CFFT approach in the BLQH with broken symmetry. We also pushed the CBFT theory further to study the instability driven by magneto-roton minimum collapsing at a finite wave-vector leading to the inhomogeneous exciton pairing state in intermediate distance  $d_{c1} < d < d_{c2}$  and quantum phase transitions between the different ground states.

In the first part of this paper, we used a MCF approach to study balanced and in-balanced BLQH systems. We achieved some success, but also run into many troublesome problems. We explicitly identified these problems and motivated the alternative CB approach. Extension of Murthy-Shankar's formalism [31] in SLQH to BLQH can not fix these problems. In the second part of the paper, we developed a simple and effective CB theory to study the BLQH. The CB theory naturally fixed all the problems suffered in the MCF theory presented in the first part. By using this CB theory, we are able to put spin and charge degree freedoms in the same footing, explicitly brought out the spin-charge connection in a straightforward way and classified all the possible excitations in a systematic way. By using this CB theory, we first studied the balanced BLQH and re-derived many previous results in a simple and transparent way. We made detailed comparisons between the spin sector of the CB theory with EPQFM derived from microscopic LLL approach. We found that although some parameters in the spin sector can only be taken as phenomenological parameters, the functional form is identical to the EPQFM. We then analyzed the instability in the pseudo-spin sector and found the magneto-roton minimum collapsing leads to a new ground state which not only breaks the global  $U(1)$  symmetry, but also the translational symmetry: inhomogeneous exciton pairing state. This state is still a QH state. It not only has the NGM, but also gapless lattice phonon modes due to the broken translational symmetry. This I-E SF state has very low critical velocity, low  $KT$  transition temperature and is very sensitive to disorders. It may lead to the excess dissipations observed in interlayer tunneling and counter flow experiments. When the distance is further increased, the minimum exciton pairing vanish, the I-E SF becomes to FL state. Because the CB approach in this paper is a phenomenological approach, if the I-E SF state is indeed a true ground state in

BLQH system need to be checked from microscopic LLL calculations which take into account the fact that the wavefunction at any finite  $d$  is qualitatively different from the (111) wavefunction [36]. Ultimately, it should be tested by experiments [49].

We then applied the theory to study the effects of imbalance on all the three states in the balanced case. We found that on the ESF and I-ESF sides, as we tune the imbalance, the system supports continuously changing fractional charges, the spin-wave velocity decreases quadratically, while the meron pair separation remains the same and the critical in-plane magnetic field for the C-IC transition increases. The critical distance  $d_{c1}$  decreases. We also derived the dual action of the CB theory in terms of topological currents and dual gauge fields. By comparing this dual action with the action derived from MCF theory, we can explicitly identify the missing and the artifacts of the MCF approach in section II. On the FL side, there could be a transition from the FL to I-ESF driven by the imbalance. But we do not have a theory to describe this possible transition. We discussed briefly the effects of disorders. We also compared our results with the previous results from LLL+HF approach, other proposals on intermediate phases and available experimental data. It would be interesting to see if the inhomogeneous exciton pairing can also be achieved in the multiple exciton pairings in Tri-layer quantum Hall systems studied in [57].

Only the interlayer coherent (111) state was discussed in this paper, it can be easily generalized to other interlayer coherent  $(m; m; m)$  (with  $m$  odd) states at total filling factors  $\nu_T = 1/m$ . For general  $(m; m^0; n)$  states with  $m; m^0$  are odd and  $m, m^0 \neq 0$ , because there are no broken symmetry in the ground states and no associated gapless Goldstone modes, we expect the Composite Fermion approach works better. For example,  $(3; 3; 1)$  state at  $\nu_T = 1/2$  can be described in terms of the Entangled Composite Fermion (ECF) discussed at section II 7.

It is general true that when there is an ordered state with broken symmetry and an associated order parameter, bosonic approach is superior than fermionic approach. Furthermore, the bosonic approach can be easily applied to study inhomogeneous state with broken translational symmetry. For example, in Quantum Antiferromagnet, fermionic approach can only address the disordered phase [53], while bosonic approach [54] can address not only the disordered phase, but also the ordered phase with broken symmetry and the quantum phase transition between the disordered phase and ordered phase. Similarly, in quantum spin glass, bosonic approach can study spin liquid, spin glass and the quantum phase transition between the two, while the fermionic representation can only study the spin liquid phase [55]. In SLQH system, there is only algebraic long range order, but no broken symmetry and no true ordered state, so CF approach

could be very successful. While  $(m; m; m)$  BLQH system has a true broken symmetry ground state and an associated order parameter and a Goldstone mode, the CB approach becomes more effective as demonstrated in this paper. Most importantly, we use the CB approach to explore the I-ESF state which could be the true ground state responsible for all the experimental observations.

As shown in [58], due to the long-range Coulomb interactions between electrons, in the effective low energy theory describing the edge reconstruction in the FQHE, there are also two low energy sectors at  $k = 0$  and  $k = k_r$ . It is the magneto-roton minimum collapsing at  $k = k_r$  is responsible for edge reconstruction in the edge state of FQHE. In one dimensional edge, the roton manifold at  $k = k_r$  becomes two isolated points. This paper showed that the magneto-roton minimum collapsing at  $d = 2$  leads to the I-ESF state. At  $2d$ , the roton manifold at  $k = k_r$  is a circle. In [61], it was shown that the roton minimum collapsing driven by pressure could lead to a supersolid state in He4. At  $3d$ , the roton manifold at  $k = k_r$  is a sphere. Combining all these results, we find that the roton minimum collapsing could lead to novel physics in all possible experimental accessible dimensions.

Inspired by recent possible discovery of supersolid in He4 [59{61], in the dual density representation of Eqn 21, we explore the possibility of excitonic normal solid (ENS) and excitonic supersolid (ESS) in the BLQH systems [62].

I thank H. Fertig, E. Fradkin, S. M. Girvin, B. Halperin, J. K. Jain, A. H. MacDonald and G. Murthy for helpful discussions. I also thank Prof. Haiqing Lin for hospitality during my visit at Chinese University of Hong Kong in the summer of 2004.

- 
- [1] B. I. Halperin, *Helv. Phys. Acta* 56, 75 (1983); *Surf. Sci.* 305, 1 (1994)
  - [2] For reviews of bilayer quantum Hall systems, see S. M. Girvin and A. H. MacDonald, in *Perspectives in Quantum Hall Effects*, edited by S. Das Sarma and A. Ron Pinczuk (Wiley, New York, 1997).
  - [3] J. P. Eisenstein, L. N. Pfeiffer and K. W. West, *Phys. Rev. Lett.* 69, 3804 (1992); Song He, P. M. Platzman and B. I. Halperin, *Phys. Rev. Lett.* 71, 777 (1993).
  - [4] I. B. Spielman et al, *Phys. Rev. Lett.* 84, 5808 (2000). *ibid*, 87, 036803 (2001).
  - [5] M. Kellogg, et al, *Phys. Rev. Lett.* 88, 126804 (2002).
  - [6] J. P. Eisenstein and A. H. MacDonald, *cond-mat/0404113*. M. Kellogg, et al, *cond-mat/0401521*. E. Tutuc, M. Shayegani, D. A. Huse, *cond-mat/0402186*.
  - [7] H. Fertig, *Phys. Rev. B* 40, 1087 (1989).
  - [8] X. G. Wen and A. Zee, *Phys. Rev. Lett.* 69, 1811 (1992).

- [9] Z.F. Ezawa and A. Iwazaki, Phys. Rev. B. 47, 7259; 48, 15189 (1993). Phys. Rev. Lett. 70, 3119 (1993).
- [10] Kun Yang et al, Phys. Rev. Lett. 72, 732 (1994). Phys. Rev. B 54, 11644 (1996).
- [11] K. Moon et al, Phys. Rev. B 51, 5138 (1995).
- [12] L. Balents and L. Radzihovsky, Phys. Rev. Lett. 86, 1825 (2001). A. Stern, S. M. Girvin, A. H. MacDonald and N. Ma, *ibid* 86, 1829 (2001). M. Fogler and F. Wilczek, *ibid* 86, 1833 (2001), Y. N. Joglekar and A. H. MacDonald, Phys. Rev. Lett. 87, 196802 (2001), Ziqiang Wang, Phys. Rev. Lett. 94, 176804 (2005).
- [13] Enrico Rossi, Alvaro S. Nunez, A. H. MacDonald, Phys. Rev. Lett. 95, 266804 (2005).
- [14] A. Lopez and E. Fradkin, Phys. Rev. B 51, 4347 (1995); *ibid*, 63, 085306, 2001. See also a review article by the two authors in Composite Fermions: A unified view of the Quantum Hall Regime, edited by Olli Heinonen. World Scientific (Singapore, 1998).
- [15] Yong Baek Kim et al, cond-mat/0011459.
- [16] M. Y. Veilleux, L. Balents and M. P. A. Fisher, Phys. Rev. B. 66, 155401 (2002).
- [17] V. W. Scarola and J. K. Jain, Phys. Rev. B 64, 085313 (2001).
- [18] S. A. Brazovskii, JETP 41, 85 (1975).
- [19] P. Fuke and R. A. Ferrell, Phys. Rev. 135, A 550?A 563 (1964).
- [20] A. I. Larkin and Yu. N. Ovchinnikov, Sov. Phys. JETP 20, 762 (1965).
- [21] Ganpathy Murthy, R. Shankar, Novel Phases of Planar Fermionic Systems, J. Phys. Condens. Matter 7, 9155 (1995).
- [22] Jinwu Ye, cond-mat/0512480
- [23] P. W. Anderson, cond-mat/9812063.
- [24] Jinwu Ye, Phys. Rev. Lett. 86, 316 (2001).
- [25] L. Balents, M. P. A. Fisher and C. Nayak, Int. J. Mod. Phys. B 12, 1033 (1998), Phys. Rev. B 60, 1654 (1999).
- [26] Jinwu Ye, Phys. Rev. Lett. 87, 227003 (2001); Phys. Rev. B. 65, 214505 (2002).
- [27] The concept of MCF was implied previously in [8,14,17] in different languages. Here, we explicitly write down the relation between a MCF and an original electron by Eqn 2 which is useful to the following developments in the paper.
- [28] J. K. Jain, Phys. Rev. Lett. 63, 199 (1989).
- [29] A. Lopez and E. Fradkin, Phys. Rev. B. 44, 5246 (1991).
- [30] B. I. Halperin, P. A. Lee and N. Read, Phys. Rev. B 47, 7312 (1993).
- [31] See the review by G. Murthy and R. Shankar, Rev. of Mod. Phys. 75, 1101, 2003.
- [32] Jinwu Ye and S. Sachdev, Phys. Rev. Lett. 80, 5409 (1998). Jinwu Ye, Phys. Rev. B 60, 8290 (1999).
- [33] S. M. Girvin and A. H. MacDonald, Phys. Rev. Lett. 58, 1252 (1987).
- [34] S. Z. Zhang, T. H. Hansson and S. Kivelson, Phys. Rev. Lett. 62, 82 (1989). S. Z. Zhang, Int. J. Mod. Phys. B 6, 25 (1992).
- [35] S. L. Sondhi et al, Phys. Rev. B 47, 16419 (1993).
- [36] Gun Sang Jeon and Jinwu Ye, Phys. Rev. B 71, 035348 (2005).
- [37] For discussions on relations between Abelian bosonization and Non-Abelian bosonization approaches to multi-channel Kondo model, see Jinwu Ye, Phys. Rev. Lett. 77, 3224 (1996).
- [38] Feynman originally conceived the 3d roton as drifting vortex loop. But this point of view is very controversial. If taking this view, then the 3d roton condensation can be considered as the vortex loop condensation. In 2d BLQH, the magneto-roton condensation in Fig. 3 may be considered as that of the charge neutral meron pairs listed below Eqn.34 and Eqn.42.
- [39] Jinwu Ye, unpublished.
- [40] For a nice review on the KTHNY theory on two dimensional lattice, see the wonderful book by P. M. Chaikin and T. C. Lubensky, principles of condensed matter physics, Cambridge university press, 1995. Note that the hexatic phase in the KTHNY theory is still not convincingly established in experiments.
- [41] M. Kellogg, et al, Phys. Rev. Lett. 90, 246801 (2003).
- [42] For discussions on Classical Lifshitz Point (CLP) and their applications in nematic to smectic-A and -C transitions in liquid crystal, see the book in [40].
- [43] For imbalanced driven quantum phase transitions in a relativistic model which treat both spin and charge sectors at the same footing, see Jinwu Ye, preprint.
- [44] C. B. Hanna, Bull. Am. Phys. Soc. 42, 553 (1997)
- [45] Y. N. Joglekar and A. H. MacDonald, Phys. Rev. B 65, 235319 (2002).
- [46] W. R. Clarke, et. al, preprint
- [47] I. B. Spielman, et al, cond-mat/0406067.
- [48] Laughlin, in The Quantum Hall Effects, 2nd ed. edited by R. E. Prange and S. M. Girvin (Springer-Verlag, New York, 1990).
- [49] For light scattering experiments, see Aaron Pinczuk, Chap. 8 in Perspectives in Quantum Hall Effects, edited by S. Das Sarma and Aaron Pinczuk (Wiley, New York, 1997).
- [50] S. Simon, E. H. Rezayi and M. V. Milovanovic, Phys. Rev. Lett. 91, 046803 (2003).
- [51] A. Stern and B. I. Halperin, Phys. Rev. Lett. 88, 106801 (2002).
- [52] Ziqiang Wang, Phys. Rev. Lett. 92, 136803 (2004).
- [53] I. A. Eck and J. B. Marston, Phys. Rev. B 37, 3774 (1988).
- [54] N. Read and S. Sachdev, Phys. Rev. B 42, 4568 (1990).
- [55] S. Sachdev and Jinwu Ye, Phys. Rev. Lett. 70, 3339 (1993). Phys. Rev. B 40, 546 (1989).
- [56] M. Peskin, Ann. Phys. 113, 122 (1978); C. Dasgupta and B. I. Halperin, Phys. Rev. Lett. 47, 1556 (1981).
- [57] Jinwu Ye, Phys. Rev. B 71, 125314 (2005).
- [58] Kun Yang, Phys. Rev. Lett. 91, 036802 (2003).
- [59] E. Kim and M. H. W. Chan, Nature 427, 225 – 227 (15 Jan 2004).
- [60] E. Kim and M. H. W. Chan, Science 24 September 2004; 305: 1941–1944.
- [61] Jinwu Ye, cond-mat/0603269.
- [62] Jinwu Ye, Possible excitonic normal solid and excitonic supersolid in bilayer quantum Hall systems, preprint.